# Comparative study between Laser and Water-jet machining of polymer composites

**Seyed Emad Alialhosseini**

Submitted to the
Institute of Graduate Studies and Research
in partial fulfillment of the requirements for the Degree of

Master of Science
in
Mechanical Engineering

Eastern Mediterranean University
September 2014
Gazimağusa, North Cyprus

Approval of the Institute of Graduate Studies and Research

Prof. Dr. Elvan Yılmaz
Director

I certify that this thesis satisfies the requirements as a thesis for the degree of Master of Science in Mechanical Engineering.

Prof. Dr. UğurAtikol Chair,
Department of Mechanical Engineering

We certify that we have read this thesis and that in our opinion, it is fully adequate, in scope and quality, as a thesis of the degree of Master of Science in Mechanical Engineering.

Asst. Prof. Dr. Ghulam Hussain
Supervisor

Examining Committee

1. Prof. Dr. Majid Hashemipour _____

2. Asst. Prof. Dr. Ghulam Hussain _____

3. Asst. Prof. Dr. Neriman Özada _____

# ABSTRACT

One of the most important group of advanced materials in Engineering is the polymer composite such as Carbon Fiber Reinforce Polymer (CFRPC) or Glass Fiber Reinforce Polymer (GFRP) which have been used in different industries including aerospace, shipbuilding and automotive. The mechanical manufacturing processes are not appropriate for shaping of Polymer Composites because these cause material damage.

In this work, two advanced of manufacturing processes named as Water-jet machining and Laser machining were employed with an objective to find the most useful one in reducing processing damages. To do so, samples of two materials (CFRPC and GFRPC) were cut employing both of the processes and then Scanning Electron Microscopy and Open Hole Tensile Test were performed on each sample.

The Scanning Electron Microscopy showed that the Laser-machined work pieces underwent melting of resin in the composite and caused delamination in the surrounding areas of cut surface. From the results of Open Hole Tensile Test, it was found that the Laser machining caused reduction in strength of GFRPC, however no such an effect was noticed for CFRPC. Water-jet machining did not pose any adverse effect on strength of either material.

In conclusion, Water-jet machining process is the most suitable method to process considered composites from perspectives of surface quality, delamination, productivity and cost.

**Keywords**: Carbon Fiber Reinforce Polymer Composite; Glass Fiber Reinforce Polymer Composite; Delamination.

# ÖZ

Mühendislikte ileri malzemelerin en önemli gruplarından biri de Karbon lifli armatür polimeri (CFRPC) veya Cam Elyaf armetür polimerdir (GFRPC). Bu malzeler havacılık, gemi inşa ve otomotiv olmak üzere farklı sektörlerde kullanılmaktadır Mekanik üretim süreçleri Polimer Kompozitlerin şekillendirilmesi için uygun olmadığı için maliyetlidir.

Bu çalışmada, Su-jet işleme ve Lazer işleme olarak adlandırılan iki gelişmiş üretim süreçleri işleme zararlarının azaltılmasında en yararlı olanı bulmak için kullanılmıştır. Bunu yapmak için, iki malzemeden (CFRPC ve GFRPC) numuneler üzerinde her iki işlemi uygulanarak kesilmiş, numuneler daha sonra Taramalı Elektron Mikroskobu ile incelenmiş, açık delik Çekme Testi ile test edilmiştir.

Taramalı Elektron Mikroskobu ile yapılan incelemeler sonucunda Laser ile işlenmiş numunelerin bileşenlerinde bileşik reçine erime olduğu ve kesilen yüzeylerinde katmanlarının ayrılmasına neden olduğunu tespit edildi. Açık delik Çekme Testinin incelemeleri sonuçlarından, lazer işlemede GFRPC kuvvetindeki azalmaya neden olduğu bulunmuştur ancak böyle bir etki CFRPC için saptanmadı. Su jeti işlemesinin malzemeye gücü üzerinde herhangi bir olumsuz etkisi saptanmadı.

Sonuç olarak, su-jeti işleme işlemi yüzey kalitesi, yüzeyin yıpranması, verimlilik ve maliyet açısından değerlendirildiğinde en uygun yöntemdir.

**Anahtar Kelimeler**: Karbon Elyaf güçlendirmek Polimer kompozit; Cam Elyaf güçlendirmek Polimer kompozit; katman ayrılmas

Dedicated to

My parents who have always been supportive of me in my whole life

my brothers

and Love of my life

Ghazal

# ACKNOWLEDGMENT

First and foremost I would like to thank my supervisor Assistant Prof. Dr. Ghulam Hussain for guiding and helping me with my master study, for his patience and sharing kindly his knowledge with me.

I also wish to thank all the faculty members at the department of Mechanical Engineering, and specially the chairman, Prof. Dr. Ugur Atikol, for providing a conductive environment during my master studies.

And also I appreciate the Cooperation of Razi laboratory of Iran, Haqshenas Company and Toos Company, which helped me in this project.

Last but not least I would like to express my grathitude to my dear friend Eng. Ramtin Nazerian who helped me a lot.

# TABLE OF CONTENTS

# LIST OF TABLES

# LIST OF FIGURES

# LIST OF SYMBOLS AND ABBREVIATIONS

| | |
|---|---|
| AFRP | Aramid Fiber Reinforced Polymer Composite |
| CFRPC | Carbon Fiber Reinforced Polymer Composite |
| CMC | Ceramic Matrix Composites |
| GFRPC | Glass Fiber Reinforced Polymer Composite |
| HAZ | Heat-Affected Zone |
| LASER | Light Amplification by Stimulated Emission of Radiation |
| MMC | Metal Matrix Composites |
| Nd:YAG | Neodymium-doped Yttrium Aluminium Garnet; Nd:Y3Al5O12 |
| Nd:YVO4 | Neodymium-doped Yttrium orthoVanadate |
| PAN | Polyacrylonitrile |
| PMC | Polymer Matrix Composites |
| UV | Ultra Violet |
| OHTT | Open Hole Tensile Test |
| SEM | Scanning Electron Microscope |

# Chapter 1

# INTRODUCTION

The importance of the composite materials in different industries such as aerospace, shipbuilding and automotive industries has encouraged me to use them in this research. These composite materials are divided into three groups including metal, polymer and ceramic, which are widely used in industries; the reason is their low weight against the high strength. **CFRPC**[1] and **GFRP**[2] are two functional samples of composite materials [1]

Most of the materials need forming and machining for industrial usages and composites are not exception of this rule. But traditional machining can result lots of damages and problems during the process. [2] [3] [4] [5]

Advanced machining technology is able to improve the quality and lead to the most feasible statement. Considering the target materials, best ways for cutting with low damage are **Laser machining** and **Water-jet machining.** These machines can reduce damage to the minimum level.

## 1.1 Thesis contribution

In this research a comparative examination between Laser machining and Water-jet machining of CFRPC and GFRPC has been carried out, and the results are compared in terms of surface quality after machining.

[1]Carbon Fiber Reinforced Polymer Composite
[2] Glass Fiber Reinforced Polymer Composite

## 1.2 Thesis Overview

Following a brief introduction in the first Chapter, Chapter 2 provides a comprehensive literature review of Laser machining and composites materials. Chapter 3 and 4 discusses about the materials and machines that used in this project.

Experimental phase explain in Chapter 5 and results and discussion have been explain in Chapter 6. Finally the conclusion has been prepare in Chapter 7.

# Chapter 2

# LITERATURE REVIEW

Researchers have done many different experiences and analyzes in the field of traditional machining on polymers materials. Although now a days, with the advances in technology and the subject of high accuracy the reduction of error after machining becomes very important. One of the solutions for this requirement is the usage of advanced machining on polymers which has been discussed in this thesis.

## 2.1 Laser and Water-jet Processes

By today, many authors have carried out several studies on Laser processing of CFRPCs. Tagliaferri et al. [6] could demonstrate that in comparison to Aramid fiber composites (AFRP) and glass (GFRP) it is much harder to obtain high quality cuts in carbon fiber composites. The reason is that there is a huge difference between the thermal properties of the matrix and the fibers in CFRPC. Furthermore, it has been found that high speed cutting can improve the cut quality. Subsequently a new thermal model with one parameter was presented by Caprino and Tagliafferi [7]. This model is able to calculate the maximum cutting speed as a function of the thickness and the energy density for AFRP, CFRPC and GFRP in continuous wave (CW) mode. There have also been some efforts to present a criterion to arrange the cut qualities. Davim et al. has studied several material composites and polymers in terms of cut quality, including cotton fibers, glass fiber, epoxy resin and phenolic resin while cutting with CO2 Laser [8]. In pulse mode, low energy input during cutting resulted cut edges with a large HAZ and burnout. Further studies abut Laser

cutting in pulsed mode was carried out by Lau et al. [9]. They evaluated a 2.5 mm thick CFRPC sheet and succeeded to find the optimum pulse duration. Although the optimum pulse duration will maximize the Laser beam penetration depth but the HAZ is directly proportional to this parameter. Hocheng and Pan [10]discovered the direct proportion of HAZ to the duty cycle of the pulse and to the peak of Laser power and its inverse proportion to the speed of cutting.

Further researches by Caprino et al. [11] indicated that it is the nature of fibers and their volumetric fraction into the composite who determines the appropriate Laser power for cutting a composite material. The dependence of the kerf size to the Laser power has been investigated by Al-Sulaiman et al. [12]. They illustrated that increasing the Laser power as well as appropriate fiber orientation will increase kerf width. As a comprehensive study Cenna et al. [13] has reviewed the Laser cutting of composites and different aspects of the process. They also suggested simulating the cutting process which will improve the cut quality because of reduction of heat-affected zone. As in previous works CO2 Laser had been mainly used and the polymeric matrix and fibers and the amount of absorption to the radiation emitted by this Laser had been nearly constant, several researchers decided to use different Laser sources with the purpose of reducing the HAZ. In order to improve cut quality in Laser cutting by Nd:YAG pulse Mathew et al. [14] made an effort to recognize the most effect parameters and regulate them optimally by a response surface methodology. A comparative study on cutting process using CO2 Laser and excimer Laser was also carried out by Dell'Erbaetal. Theexcimer Laser providing UV radiation resulted the best cut quality however the productivity was too low. The quality of CFRPCs composites processed by use of a third-harmonic Q-switched Nd:YVO4 Laser has also been investigated by Li et al. where they set the emitted

UV radiation at 355 nm. They discovered that it is possible to achieve cuts with minimum HAZ by a very time consuming process [15]. In another comparative study, Herzog et al. [16] focused on the relation between Processing conditions and the HAZ extension as well as the static strength. In this experiment a disk Laser, a pulsed Nd:YAG Laser and a CO2 Laser were used to cut a CFRPC specimens of 1.5 mm thickness. Results showed that the HAZ extension is lower in Laser cut by Nd:YAG. Some kind of correlation between the static strength and the HAZ extension was also discovered. ; Work pieces with less HAZ extension processed by Nd:YAG Laser had larger values of bending strength and static tensile. Further efforts by Chryssolouris et al. [17] to reduce the HAZ extension introduced the use of a non-coaxial Water-jet during Laser grooving. In another CO2 Laser cutting experiment on CFRPC plates, Jaeschke et al. [18] introduced a new method to fill the voids caused by the vaporized matrix. They succeeded to achieve a maximum degree of sealing about 85%. They suggested using an extra polyamide powder (PA 6 powder) to ‘‘heal’’ the structure after Laser cutting.

All these studied introduced CO2 Lasers as the best candidate to process CFRPC composites. Nowadays, high output power and high-quality beam of CO2 Lasers has allowed them to be used in more than 40,000 cutting machines all around the world. These Lasers are widely in charge to cut several sorts of materials such as ceramics [19], metals [20] [21] or polymers [22] [23]. Unlike other wavelengths of Laser radiation, the CFRPC fibers composites and the polymeric matrix highly absorb the k = 10.6 lm Laser radiations.

Water-jet machining on composite materials has also been the objective of many researches. J. Wang has crried out two researches titled " Abrasive Waterjet

Machining of Polymer Matrix Composites” and " Predictive depth of jet penetration models for abrasive waterjet cutting of aluminia ceramics” [24] [25] , Hashish M, has also studied the " Status and potential of waterjet machining of composites" [26], Momber A.W, presented " Principles Of Abrasive Water-jet Machining" [27], Mahesh Haldankar, has worked on "Experimental and FEA of particle impact erosion for polymer composites" [28], A Alberdi, has researched about " Composite cutting with abrasive Water-jet” [29], E Leema, publishd a paper titled “Study of Cutting Fiber-Reinforced Composites by Using Abrasive Waterjet with Cutting head Oscillation” [30].

## 2.2 Thesis Statement

According to the geometric shape of the instruments and traditional machines, as we have mentioned in literature review, amount of damages in traditional machines are much higher compared to advanced machines. The reason is the high cutting precision in advanced machines.

Due to adoption of polymer materials, machines used in this project are Laser and Water-jet. This project targets to optimize the surface quality after machining which can be achieved by using advanced machines.

The goal of this research is comparing the surface quality of material after Laser and Water-jet Machining.

# Chapter 3

# COMPOSITE MATERIALS

The new generation of composites materials which are known as a class of advanced materials, contain some simple materials to provide some superior mechanical and physical properties. Parts keep their own features and will not be solved or mixed. Using these kinds of materials has also been popular in the past. As an example ancient people used composites in building construction and they utilized fiber as reinforcement. When resin and fiber are mixed together and form a baked brick they are more stable than when they are apart. Nowadays in numerous industries such as space, reactor building, electronic and etc. usual and known materials cannot supply all the needs, but composites can be really helpful for these cases.

## 3.1 Definition of composites

Usually composites are defined as a microscopic physical mixture of several substances which keep their own features and boundaries. This mixture provides more desirable properties compared to each of the components. In composites there are generally two distinct areas as following. [1]

1. Continues phase (Matrix)
2. Discontinuous phase (reinforcement)

In a composite material, fiber is the important section for load while the matrix is the factor to transfer the force to the whole area equally besides it will save the

composite against the high temperature and humidity [1]. Composite materials can be classified in three groups as described in figure 3.1.

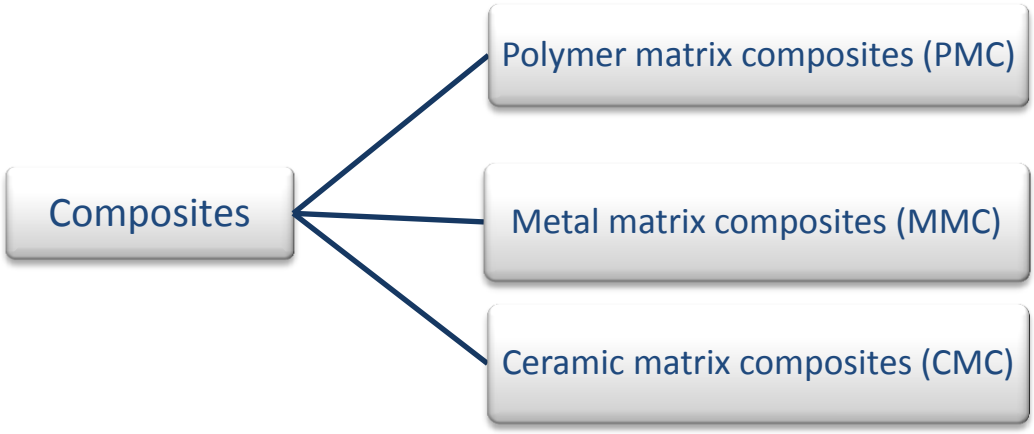


Figure 3.1: Classification of composite materials

### 3.1.1 Polymer Matrix Composites (PMC)

Polymer matrix composites are made up of a polymer resin as the matrix and reinforcement strings. Different features of PMC materials including perfect properties in room temperature ease of construction and low cost have made them to be used in a wide variety of applications. These composites are classified based on their reinforcement in three groups as Glass, Carbon and Aramid. In the future Carbon will be more popular than glass for the reinforcement strings. The reason is its highest strength among all other materials.

### 3.1.2 Metal Matrix Composites (MMC)

In metal matrix composites, the matrix is made up of a flexible metal. The advantages of these composites compared to polymer composites are the better performance in higher temperatures, non flammability and the more resistance against fluid. However they are more expensive and also their usage is more limited than polymers.

Aluminum-Magnesium alloys and Titanium-Copper alloys are two different sorts of super alloys which can be used as the matrix. The reinforcements can be used as particles, continuous or non-continuous fibers or whisker which make up 10 to 60 percent of the weight of components. As an example some components have been made by Aluminum alloys.

Recently, automakers have used some metal matrix composites in their motor's matrix with Alumina and Carbon strings which has resulted lighter weight and more resistance against fraction and high temperature. Besides metal matrix composites have found their way into aerospace industries such as the construction of Hubble space Telescope.

### 3.1.3 Ceramic Matrix Composites (CMC)

The excellent resistance to oxidation of Ceramic Matrix Composites has introduced them as the best candidates for high temperature and intense tension applications. However they have a possibility of brittle failure. By these features they can be very helpful in motor components of vehicles and gas turbines for aircrafts. The toughness of new generation of ceramic matrix composites has been increased and reached at six ( $\mathrm{MPa}\,.\,m^{\frac{1}{2}}$ ). If a crack is created in the matrix not only it will not spread, but

also particles or fibers will prevent the progress of the crack. Ceramic composites are created by hot press and ISO static press. C and Si whisker-reinforced alumina are utilized as the cutting tools in machining for hardware steel alloys.

## 3.2 Cabon Fiber Reinforce Polymer Composite

Carbon fiber is a fiber containing at least 90% Carbon and controlled paralyzing. The phrase “graphite fiber” is used when the composite has more than 99% Carbon. There are several types of fibers used as matrix and each type has some exclusive features. The most commonly used matrix fibers are Poly acrylonitrile fibers (PAN), Cellulosic fibers, coal tar pitch and an exclusive type of phenolic fibers [31]. Figure 3.1 depicts CFRPC texture.

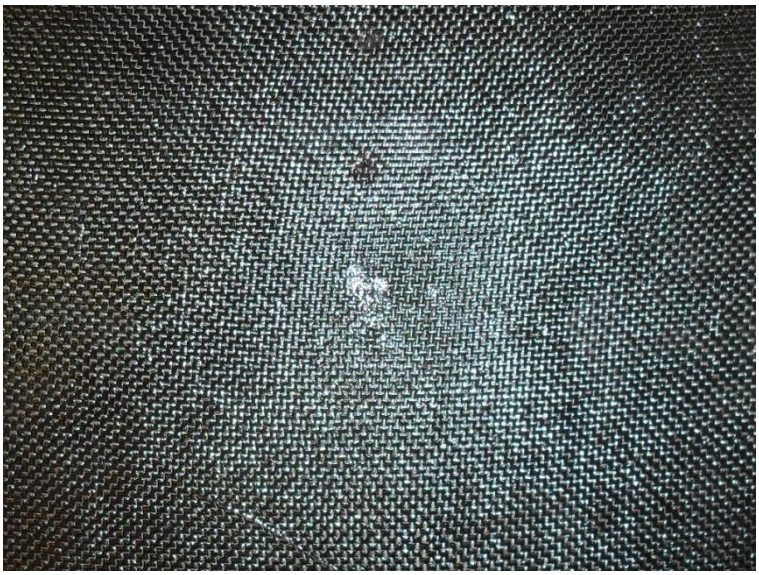

Figure 3.2: Cabon Fiber Reinforce Polymer Composite

Carbon fiber has been made by paralyzing the organic matrixes similar to fiber. In fact thermal operations removes oxygen and hydrogen thus Carbon fibers remain. Researches on Carbon [32] [15] [33] shows that the mechanical properties of Carbon will improve by increasing the crystallinity temperature and the degree of Carbon’s fibers orientation. The best solution to produce arbon fibers with adequate properties

is to use the matrix fibers with the best degree of orientation and protecting them by applying tension during the Carbonization and stabilization processes.

### 3.2.1 Carbon fiber with Poly acrylonitrile matrix production

The production steps of high quality Carbon fiber with Poly acrylonitrile matrix, are as following.

#### 3.2.1.1 Oxide stabilization phase

In this phase by applying tension PAN fiber goes under the oxide thermal operation with the temperatures of $200^{\circ}$ -$300^{\circ}$ C . This operation changes PAN to ladder or ring structure.

#### 3.2.1.2 Carbonization phase

After oxidization, Carbon fibers will be put under the $1000^{\circ}$ C in the Neutral environment (usually nitrogen) without applying any tension for a couple of hours. During this process the non-Carbon elements will be released and carbon fiber will achieve form the PAN over 50% than the start. [34]

#### 3.2.1.3 Graphitization phase

Graphitization phase depends on the Carbon fiber in terms of elastic modulus. Applying the temperature range between $1500^{\circ}$- $3000^{\circ}$ C it will result the improvement of the Carbon crystallites orientation degree in the direction of fiber and then the improvement of features.

In some way Carbon fiber production with other matrixes has the same steps as mentioned.

CFRPC used in this experiment has the following conditions as presented in Table 3.1 and 3.2 :

Table 3.1: Mechanical Properties of Carbon Fiber

| Weight | Meshing | Young modulus |
|---|---|---|
| 200 (gr) | 200 | 30 (GPa) |

Table 3.2: Resin Properties

| Resin epoxy | Weight | Hardener |
|---|---|---|
| 5052 | 100 (gr) | 25 (gr) |
| Cold bake in room temperature | Time for resin to become inundated | Sell time |
| Until 28$^{o}$C | 3-25 hours | 30-45 min |

Note that carbon fibers are non-woven.

### 3.2.2 Carbon fiber structure

Structure properties of Carbon fiber are mostly analyzed by electron-microscopes and X-ray diffractions. Unlike graphite, the Structure of carbon has no three-dimensional order. In PAN matrix carbon fiber the Structure of fiber will change from chain to layer Structure during the oxide stabilization, carbonization and graphitization processes. Thus, at the end of the carbonization, the main layers will be placed in the direction of the long axis of the fiber. Long angle X-ray studies suggest that by increasing the carbonization process temperature, accumulation height and orientation degree of the main layer will be increased too. The diameter of the filaments menu has a major influence on the penetration of carbonization in the carbon fiber. For this reason, changes in shall and core Crystallographic of each filaments menu, which is completely stabilized, are so clear. Shall has high long axis orientation with highcrystallites accumulation, however, the core shows low orientation with low crystallites accumulation. [35]

Generally, it has been observeded that as the tensile strength of matrix fiber is increased, tensile strength of the Carbon fiber will also be increased. If the stabilization phase is done properly, the tensile strength and elastic modulus will progress greatly in the final product. Observations by microscopes and X-ray diffraction machines, show that in Carbon fiber with high elastic modulus, the crystallites are located on the longitudinal axis, while the layers are settled with the most common orientation parallel to the fiber axis. In sum, Carbon fiber strength depends on the type of matrix, process condition, thermal properties temperature and Carbon fiber structural flaws. In Carbon fiber with PAN matrix, the increase of temperature until 1300℃ will increase the strength, but after 1300℃ the strength will decrease slightly. This matter is the same for elastic modulus.

Carbon fibers are so brittle. Fiber layers are attached to each other by the weak Wan Der Waals connections. Scaly accumulation of layers easily causes the crack growth in perpendicular direction to the fiber axis. In bending, fibers will break in very low strain. Despite all of these disadvantages, Carbon fibers in terms of total mechanical, chemical and physical properties has no competitors in many fields of engineering and science of these two recent decades. [32]

### 3.2.3 Applications of Carbon fibers

Carbon fibers are used in various industries. we mention some of them in this section.

#### 3.2.3.1 Transportation industry

LPG tangs for cars, engine components, shock absorber, transmission shafts, brake pads, bodies of racing cars and ship hulls are some examples of Carbon fibers usage in transportation.

#### 3.2.3.2 Building and construction industries

As examples of using Carbon fibers in building and construction industries we can mention Structural materials for bridges, bridges folding mechanism, high-strength reinforced concrete,dividing walls, using for repair the building being destroyed, using for Tunnel lining to prevent the shedding and using in the ramps for avoiding soil shedding. [34]

#### 3.2.3.3 Aerospace and aircraft industries

Passenger cabin structures including panels of chairs and tables, covers, satellites structural components, Fighter aircraft flaps, the tip of supersonic aircrafts, long-range missiles nozzles and Critical parts of aircraft engines can include Carbon fiber [32].

#### 3.2.3.4 Medical industries

Carbon fiber has been used in the construction of artificial bone, components of X-ray equipment, wheelchairs, Types of prosthetic body parts for disabilities and even heart valve.

#### 3.2.3.5 Energy sector

Carbon fibers are used in fuel batteries, Turbine blades and wind mills blades to generate electricity from wind energy.

#### 3.2.3.6 Electronics, electrical equipment, and machine building

Applications of Carbon fibers in electronics include laptop frames, computer hardware components, Industrial robot arms, gears, rollers, high speed gears, self-lubricating parts,Antennas, Electrical insulating materials, Pressure Vessels, printer rollers and mobile frames. [32]

## 3.3 Glass Fiber Reinforce Polymer Composite

The fiber used in this composite is the production of SC-Interglas with E92125 business code. This carbon fiber woven fabrics can be classified in two groups namely sleave fiber and textured fiber. These fibers are plain weaven roving with 0.25 millimeters approximate thickness. Fabric used in composite layers is shown in Figure 3.2 .

Figure 3.3: Glass Fiber Reinforce Polymer Composite

Mechanical properties of E92125 fiber are presented in Table 3.3.

Table 3.3: Mechanical properties of E92125 fiber

| Type of materials | density | Young modulus (GPa) | tensile strength (GPa) | ultimate strain (%) | Fiber diagonal (μm) | Cost $/kg |
|---|---|---|---|---|---|---|
| E92125 | 2.5 | 80 | 3.2 | 4 | 10-16 | 3 |

Th second main part of a composite is resin. Resin means the polymer used as matrix or Continuous phase of composite. One of the important heat polymers is epoxy resin. Resin used in this research is epoxy "made by Huntsman Company with Araldite LY5052 business name" with amine hardener. This resin is one of the high performance epoxies often used for construction of component with high mechanical properties such as airplane components, sport tools, automotive and maritime industries. [34]

Resin is a clear liquid, with density of 1.16-1.18 (g/cm3) at 25ºC. Other physical properties of LY5052 resin are mentioned in Table 3.4.

Table 3.4: Physical properties of LY5052 resin

| Properties / Sintering condition | Tensile strength (GPa) | Elongation (%) | Tensile modulus (GPa) | Bending strength (GPa) | Bending modulus (GPa) | Coefficient Poisson | Fracktion energy ($J/m^2$) |
|---|---|---|---|---|---|---|---|
| 15 hours in 50ºC | 82-86 | 3.5-5.5 | 3450-3650 | 126-128 | 2950-3000 | 0.35 | 202+10 |
| 7 days in room temperature | 49-71 | 1.5-2.5 | 3350-3550 | 128< | 3000< | 0.3 | ----- |

Amine hardener HY5052 is a clear liquid, with density of 0.93-0.95 (g/cm3) in 25ºC, 40-60 (mPa/s) Viscosity with the amine-rate of 9.6-9.8 (Eq/kg).

The process of composites forming is classified by different methods. Some of them classifies them in two groups of manual and machining procedures, but most of the methods divide the processes into open mold and close mold. Manual padding is the most suitable process for limmited productions and it includes polishing the male and female part of the mold, applying the separator film, putting the fiber layer and

putting resin. To produce this composite useing some continual separator materials; there is no needs to put separator film for molding.

### 3.3.1 Steps of composite production

62% of resin epoxy LY5052 with 38% of stiffener must be admixed and then become completely homogen. Clean male and female of the mold should not have any offal and corrosion. All surfaces must be soft sanded. The female mold is placed on the table and all internal surfaces and edges are covered by white separator wax. The thickness of the layer must be between 0.4-0.5 millimeters. After putting a separator, the mold will be covered by a layer of mixed resin and hardener. Then a layer of fiber, which has been cut through the certain dominations, is carefully posed in to the female mold and then it is covered by a mixed layer of resin and hardener. Afterwards the second layer of fiber is added. This process continues until the tenth layer. Subsequently the resin and hardener layers are weared and then the male mold is added on top of it. In the manual method fiber constitutes 29-33 percent of the composites weight. After these steps the mold should be placed in 22ºC for 24 hours until the baking become complete. These ten layers will achieve 2.5±0.2 millimeters. [32] [34]

Extraction of components from the mold can be easily done. Handle abrades the surfaces of the components by soft sand paper. The tensile modulus in the direction of the fibers is achieved based on the materials standard methods test (ASTM3039). This standard and its samples, are shown on Figure 3.3. The average tensile modulus is about 51 (GPa). [31]

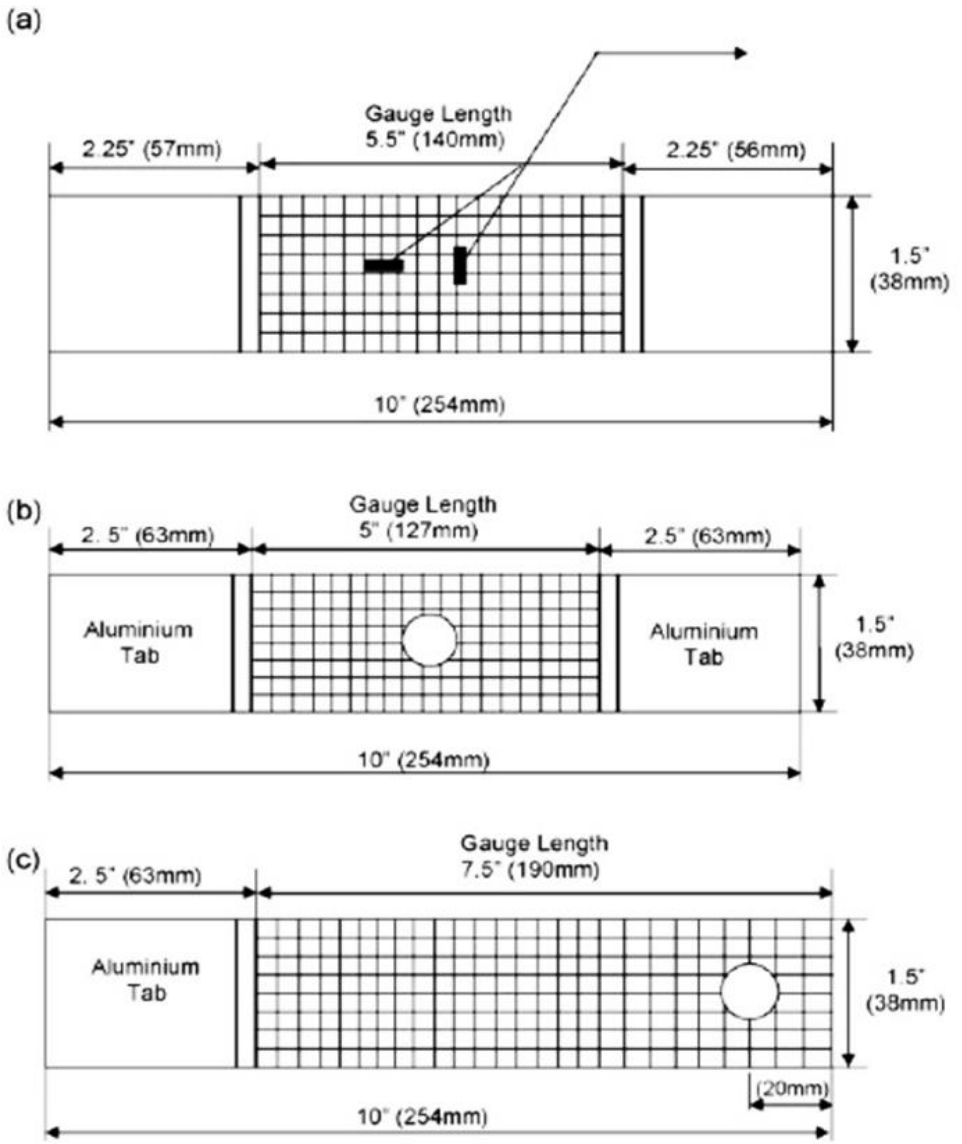


Figure 3.4: Tensile modulus in the direction of the fibers achieved based on the materials standard methods

# Chapter 4

# LASER AND WATER-JET MACHINES

## 4.1 Laser machine

What top manufacturers need in a Laser machine to remain competitive is to afford the finest Laser cutting system for every manufacturing requirement with the ability to manufacture high-quality components efficiently and cost successfully.

Amada created the LC-F1 NT after carefully analyzing this need. Founded on a complete knowledge of manufacturers' requirements, Amada has developed the new generation of advanced Laser cutting systems – the user-friendly and applications-oriented LC-F1 NT. Figure 4.1 illustrates the five inovations attend through front-loading developments.

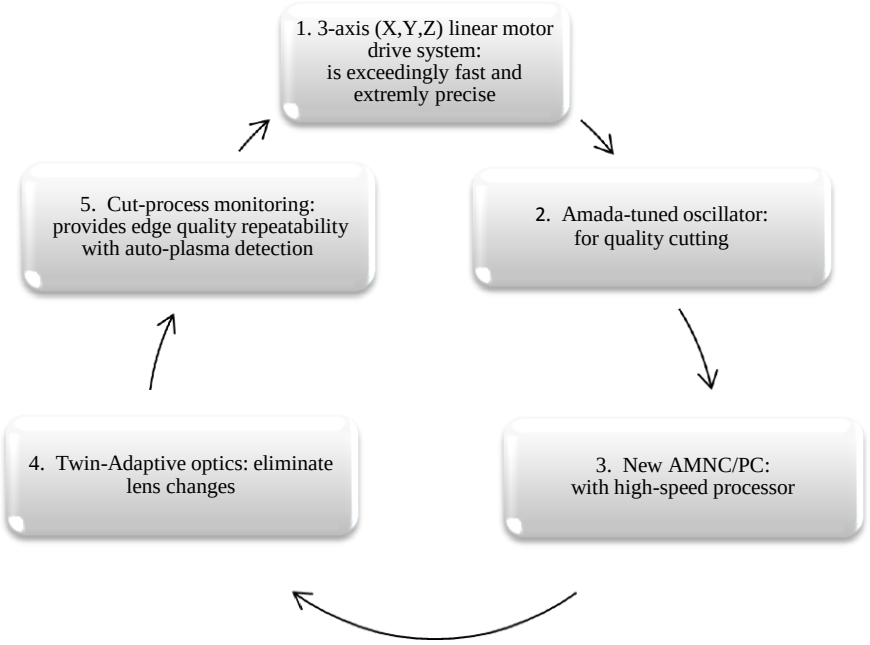


Figure 4.1: Five innovations attained through front-loading developments

### 4.1.1 Advantages of the F1

In this section we mention some advantages of the F1 which has changed the consept of Laser machine.

- Extremely Fast Piercing and Cutting by 3-axis Linear Motor Drive System.

Faster processing time speeds up NC processing which results an impressive decrease in piercing time. The joint speed of the AMNC control and the faster processing speed of the F1 significantly reduces the general processing time. Processing time for the nested area shown in Figure 4.2 is decreased approximately twice (1.89) compared to traditional machines. The effectiveness of the AMNC control has decreased the costs over 56 percent.

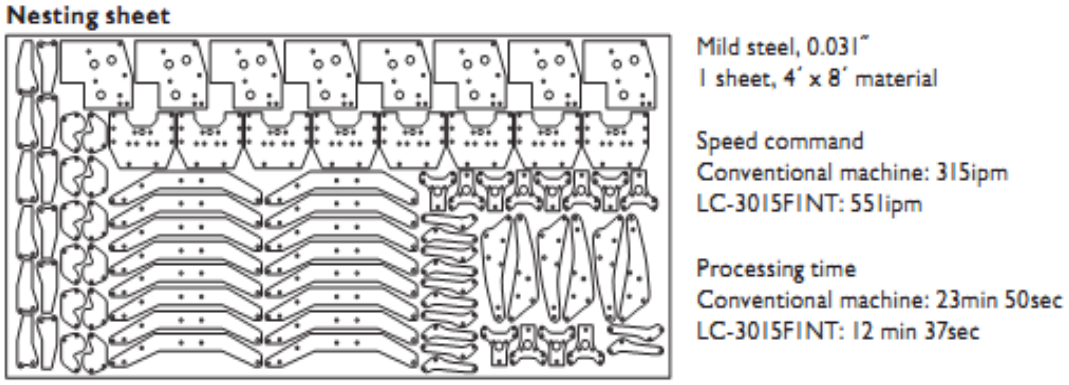


Figure 4.2: Nested area

$F_1$Laser machines can process in a shorter time in an equal cut command speed. A faster travel speed plus a faster axial acceleration/ deceleration can reduce significantly the production process. [35]

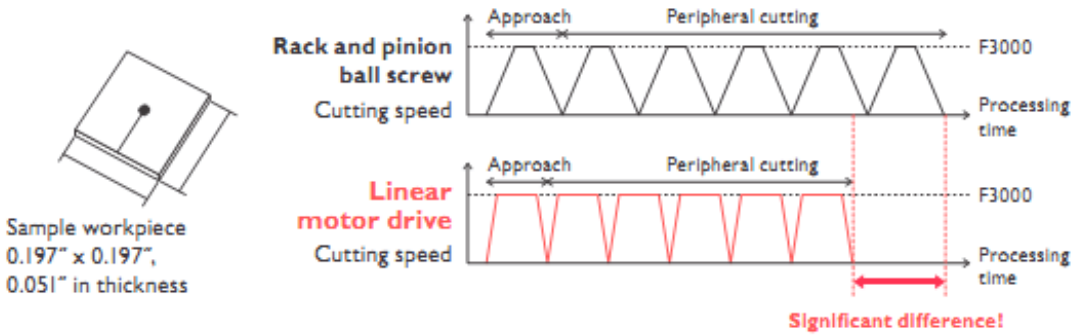


Figure 4.3: Cutting command speed, acceleration and cycle time (The time from the beginning to end of a series of operations in a single process.)

- Minimizing the beam fluctuation.

Minimizing the light fluctuation unique to a very fast axial flow improves the Laser beam quality. Furthermore the cut surface will be smoother and burn free corners and edges can be achieved [29].

Table 4.1: Comparison of cut surface quality with conventional machine. Processing speed (ipm) comparison of cut surface roughness: Ra value (µm) 0.04" top of face sheet (µm)

| Processing | | 4kW oscillator (AF4000E) on conventional machine | 4kW oscillator (AF4000I-B) on LC-FI NT |
|---|---|---|---|
| Material thickness | Assist Gas | Cut surface thickness | Cut surface thickness |
| Stainless steel | Nitrogen | 315"/min Ra=2.1 | 334.6"/min Ra=1.4 |
| Stainless steel | Nitrogen | 118.1"/min Ra=1.9 | 118.1"/min Ra=1.2 |
| Stainless steel | Nitrogen | 78.7"/min Ra=2.5 | 78.7/min Ra=1.4 |
| Mild steel | Oxygen | 118.1"/min Ra=2.2 | 118.1"/min Ra=1.1 |

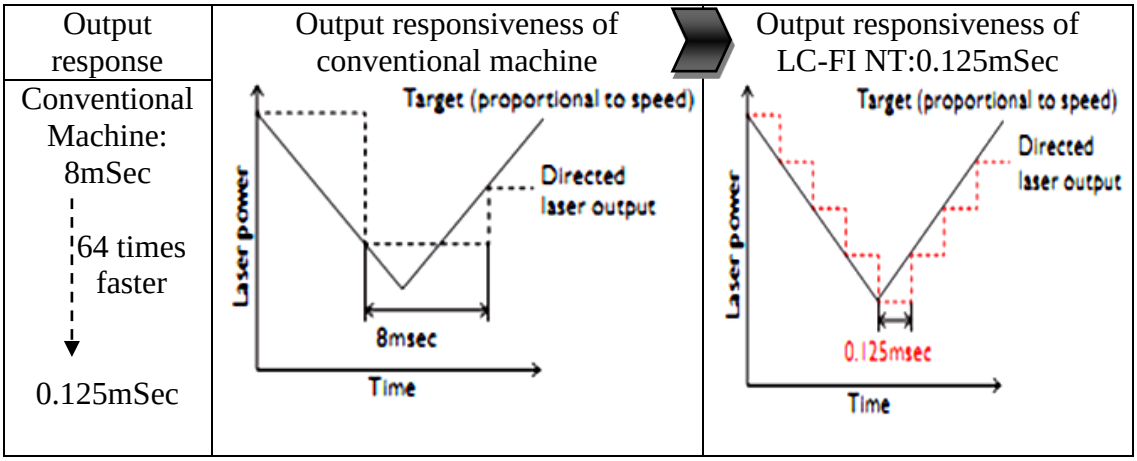


Figure 4.4: High-output sensitivity of 0.125msec with LC-F1 NT oscillator allows thorough control of Laser power

- Extraordinarily Precise**.**

Gaining high-accuracy and high-speed cutting is another excellence of this machine. A key factor in the LC-F1 NT's design is a 3-axis linear motor drive system, which allows a remarkable high precision – enabled by factual closed-loop feedback of the head site straight to the NC control. [35]

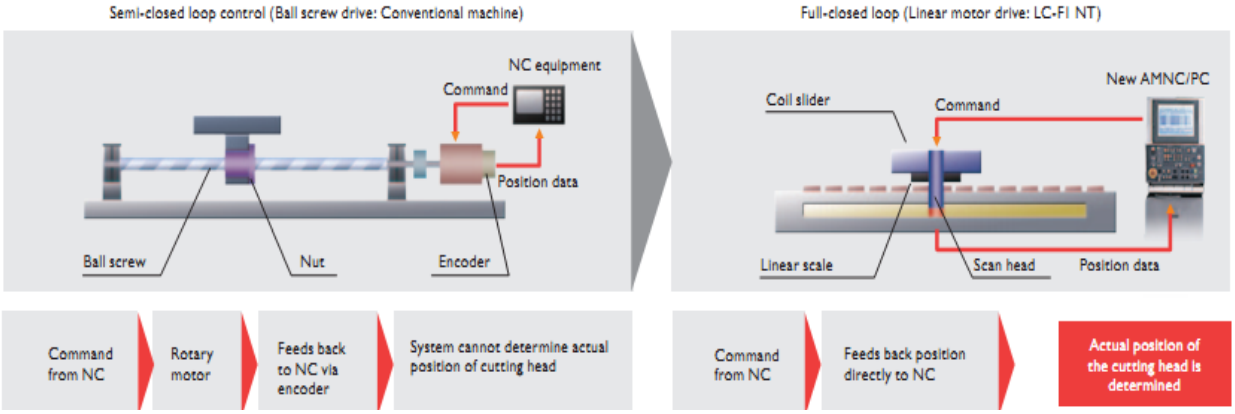


Figure 4.5: Laser Machine structure

There is a linear drive system to supply high-speed processing and reliable precision cutting. A 3-axis linear motor drive system achieves high circularity without axial wear and tear. Figure 4.6 depicts the Trajectory data of D300 (11.8″) uniform circular motion (comparison with conventional machine).

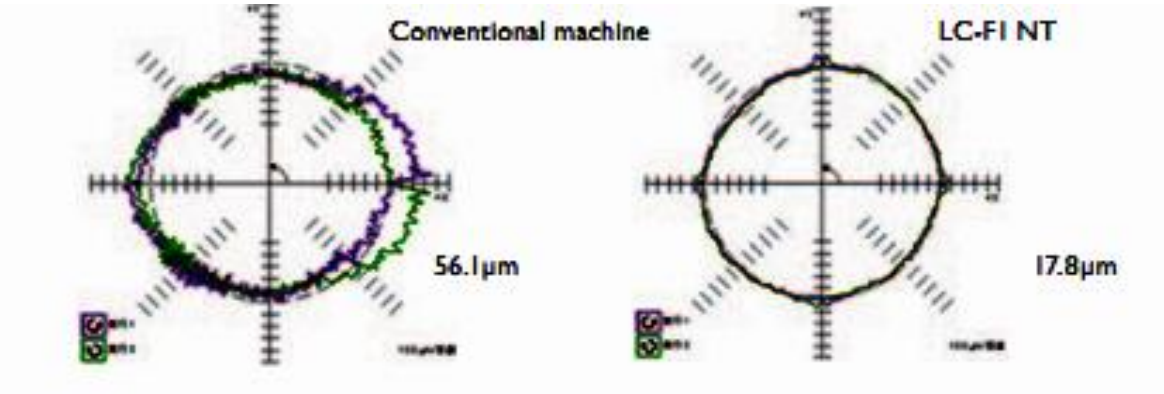


Figure 4.6: Measurement trajectoriesat 787″/min

There are two adaptive optics which manage the beam diameter for the best possible cutting performance. A single 7.5″ lens handles thin to thick layers, decreasing the costly time of replacing the lens.

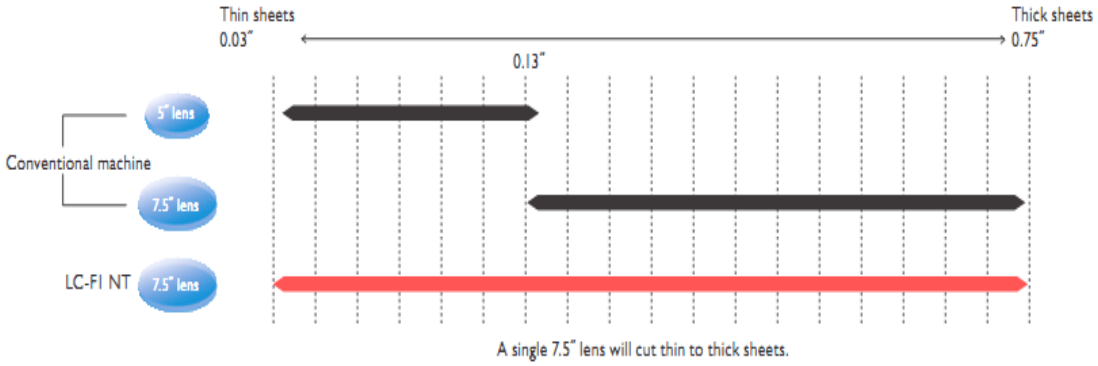


Figure 4.7: Different lens sorts and their effects on cut thickness

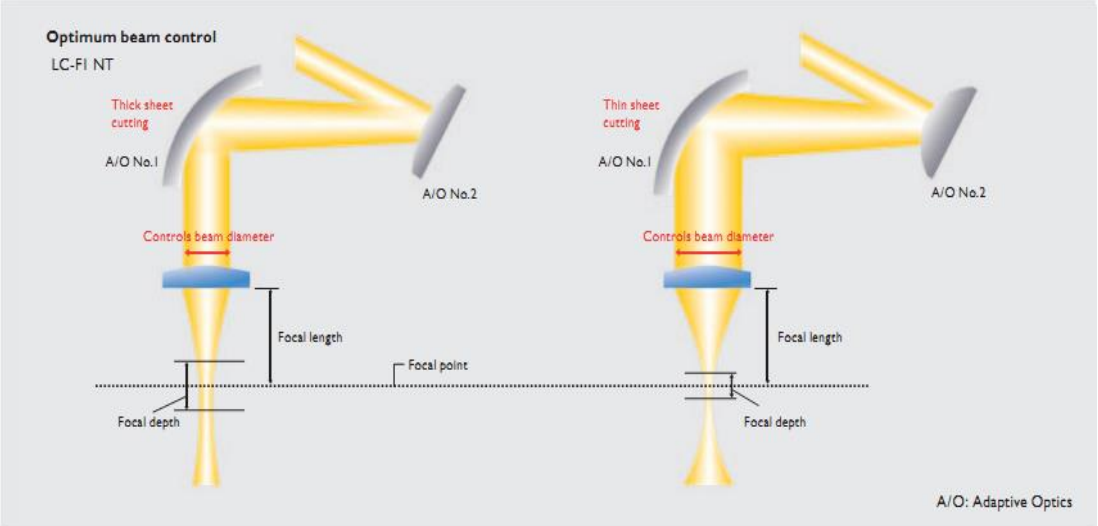


Figure 4.8: Beam control system

- Repetitive Production on Mixed Variant Material and Thickness.

The best nozzle changer supports in promotes continuous, unattended operation. An 8-station changer force automatically change, clean and calibrate both nozzle and head, based on the needs specified for the objects to be processed. This qualityraises machine utilization, while dropping overall process time. [35]

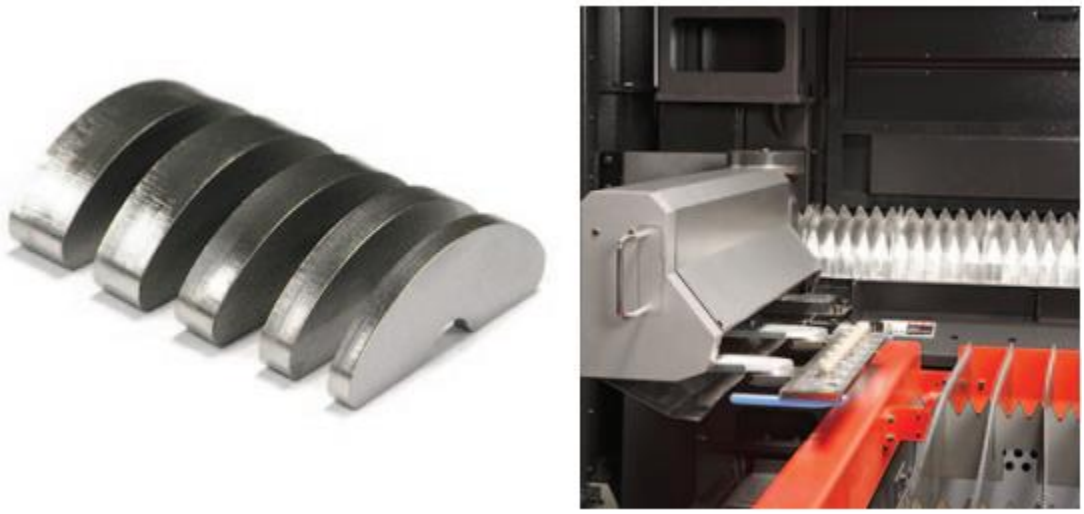

Figure 4.9: Automatic nozzle changer

- Cut-process Monitoring Automatic nozzle changers

Receiving feedback from the machine, $F_1$ Laser monitors the cut status and also displays simultaneusly cut error factors including gouging, plasma and piercing. [35]

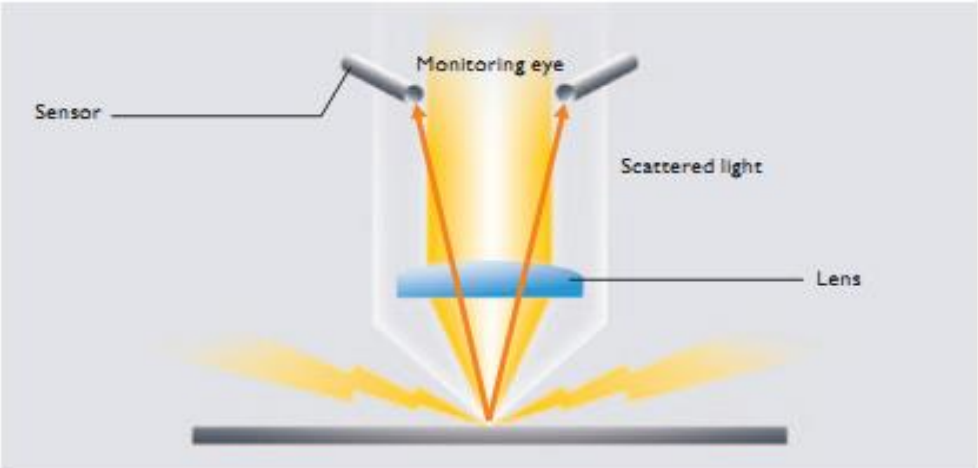


Figure 4.10: Cut status detection function

### 4.1.2 Machine Specifications

Table 4.2 contains the specifications of the Laser machine**.**

Table 4.2: Laser machine specifications

| **Model** | **LC-3015F1 NT** |
|---|---|
| Max. axis travel | 120.9" × 61" × 3.9" |
| Max. mass of load | 2.028 lbs |
| Rapid traverse | X,Y,Z: 4.724"/min |
| Max. cutting speed | 2.362"/min |
| Acceleration | X,Y:1.5G Z:3G |
| Cutting lead | Cartridge-type cutting head |
| Z-axis sensor | HS-2007 (Anti-plasma, noise resistant) |
| NC | AMNC/PC |
| Oscillator model | AF-4000I-B (4kW) |
| Power requirement | Machine:51 kVA/ Oscillator: 55 kVA /Chiller: 27 kVA |
| Machine weight | 28.660 lbs (including oscillator) |
| Standard equipment | Full opening enclosure, CNC assist gas control (2.0MPa), CNC focus control, Oil shot, Cut process monitoring, Nozzlr cleaner |

## 4.2 Water-jet machine

Water-jet machine is a device for cutting metals, rocks and some kinds of ceramics. A really thin flow of high pressure and fast water (for example 400 MPa) or water and some abrasive substances like aluminum oxide or garnet this device enables the machine to cut a wide range of materials.

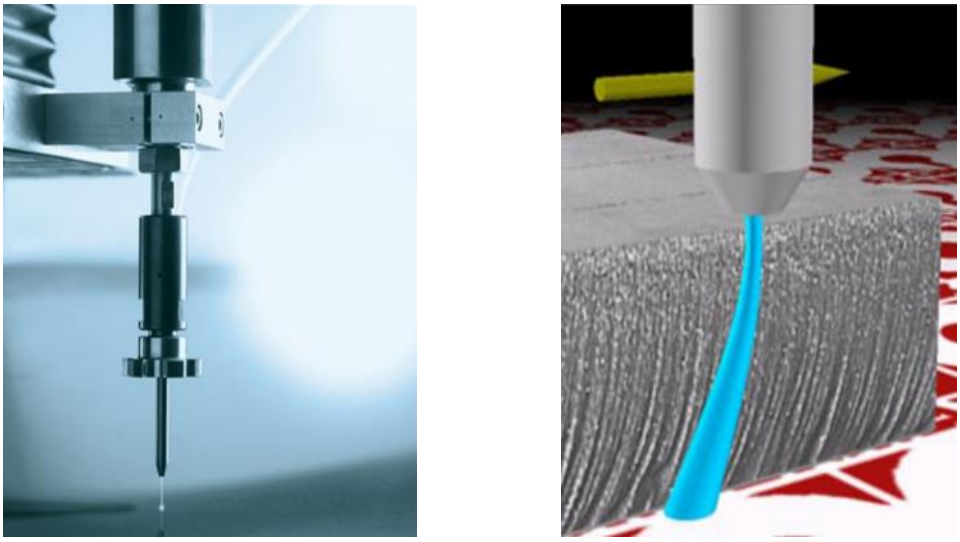

Figure 4.11: Water-jet nozzle

This machine is specially suitable for the conditions that the low temperature is necessary. Soft materials such as ladder or foam can be cut just by water.

Changing the nozzle components and type or amount of the abrasive substances, we can change the width or kerf of cutting. In normal cutting with abrasive substances, the width of cutting is between 1.016-1.27 millimeters and it can be reduced to 0.508 millimeter. But without any abrasive substances, kerf is between 0.187-0.33 millimeters. Although it can be reduced even less than 0.076 millimeters which means as thin as human's hair.

### 4.2.1 Advantages of Water-jet machine

The most remarkable advantage of waterget machine is the ability of cutting without any damage in mechanical properties of materials. This machine prevents the workpieces to tolerate the high temperature process of machining. Another advantage of this machine is its capability to cut the complicate shapes with higher quality and in lower time. This can be done by three-dimension levers and softwares.

Considering the size of nozzles, Water-jet has a low intake of water (0.5-1 Gallon per minutes). This amount of water is also recyclable. Abrasive substances are natural and recyclable too. They are also non-poisonous. The machine also will not produce dust from the machining operation. It is also important to mention that materials like tempered glasses, diamond and special ceramics can not be cut by Water-jet.

### 4.2.2 Main cutting specifications

- Usage of high speed flow of abrasive substances in the water with a very high pressure (30000-90000 Psi or 207-621 MPa)
- Cutting a wide range of different materials such as soft, hard or sensitive to the temperature
- No thermal damages in the surface or edge of the workpiece
- Nozzles are usually made from Sintered Boride
- Resulting a less than 1 degree cutting angle in most cuts which can also be avoided by decreasing the speed of process
- Space between nozzle and workpiece can affect the width and rate of cutting. It usually must be 3.175 millimeters.[30]

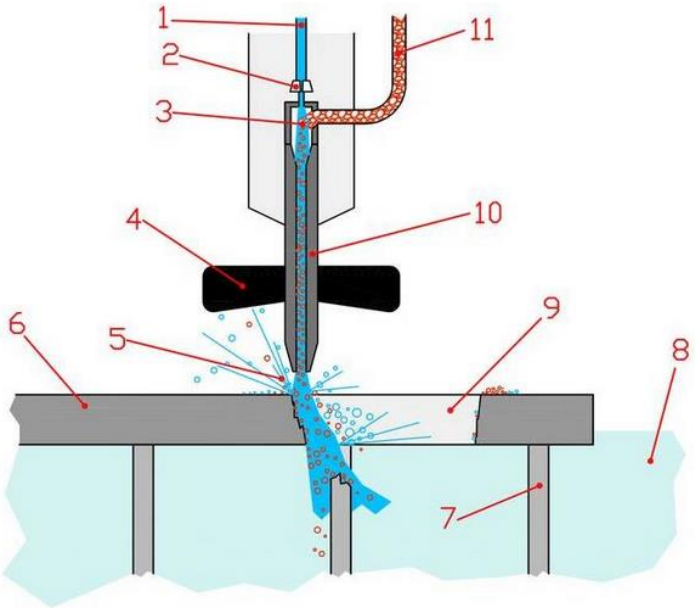


Figure 4.12: 1-Water 2-Diamond 3-Abrasive substances 4-Fixture 5-Water exit 6-Workpiece 7-Holder foundations of work piece 8-The accumulated water 9-Cut area 10-conducting pipe of water 11-Abrasive substances

### 4.2.3 Quality of surfaces or edges

Reducing the speed of cutting process the quality of the surface will improve. According to Figure 4.12, the speed of thin workpieces to reach Q1 is three time faster than Q5 and for thicker workpieces it will reach to six times faster. For example for 4 inch thick aluminum and the Q5 quality, the speed is equal to 18 millimeter per minutes and for Q1 quality the speed is 107 millimeter per minutes. [36]

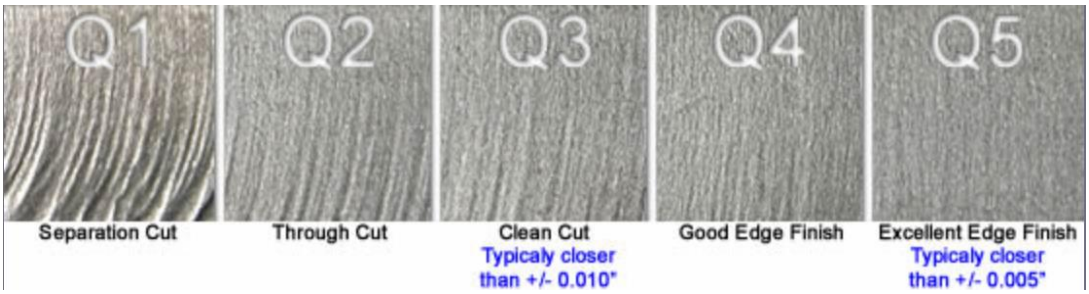


Figure 4.13: Surface quality

# Chapter 5

# EXPERIMENTAL WORK

In previous chapters machining techniques and composite materials have been explained. This chapter provides details about the effect of Water-jet and Laser machining on the mentioned materials.

At first target materials have been machined by Water-jet and Laser to become standard samples for testing. The standard for open hole tensile test is ASTM D5766 / D5766M. Figure 5.1 depicts the Dominions of samples:

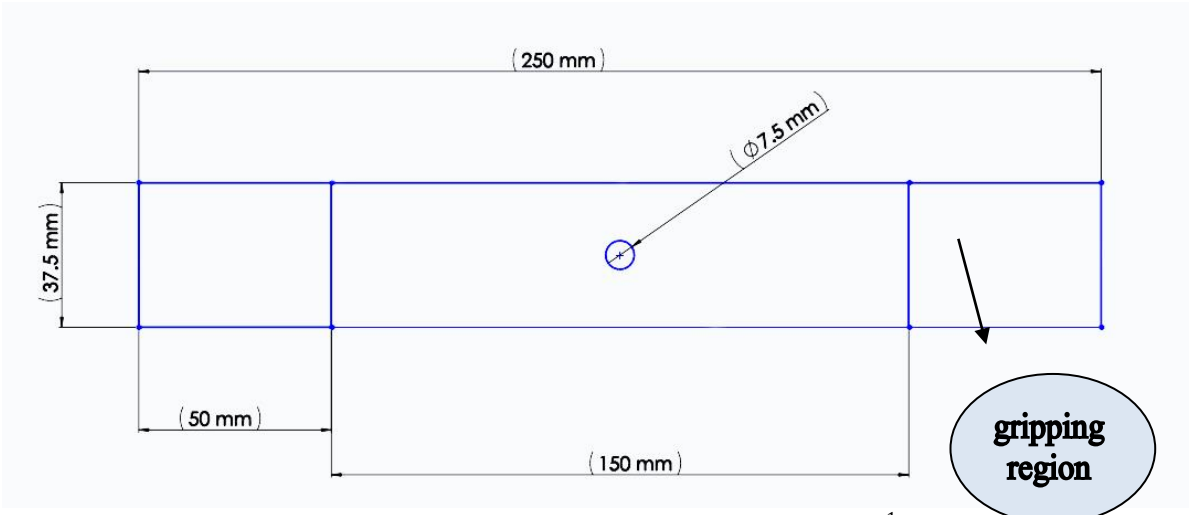


Figure 5.1: Sample of Open Hole Tensile Test (OHTT)[1]

Figure 5.2 illustrates the classified preview of the experiments done on samples.

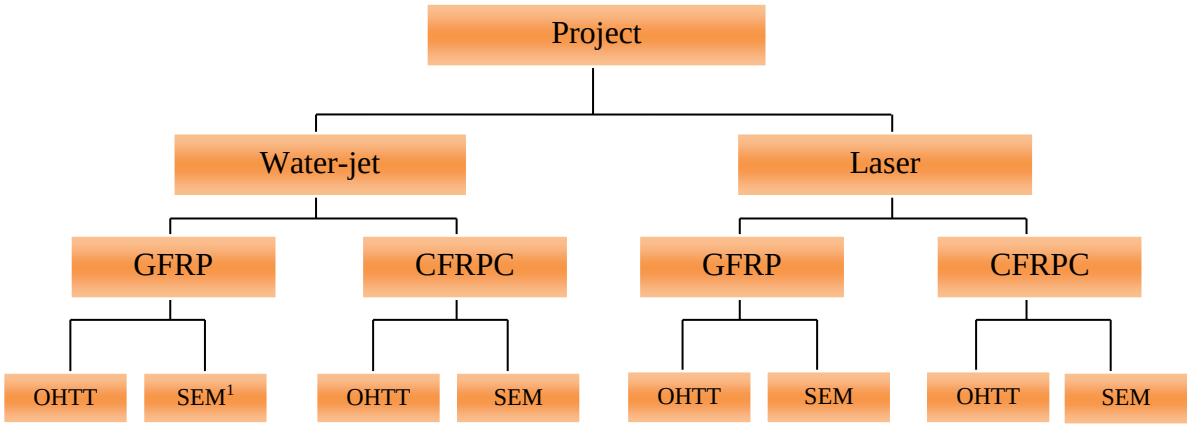

Figure 5.2: Project review

In this project CFRPC and GFRP materials are processed by Water-jet and Laser machines and the results are evaluated under two different tests namely Open Hole Tensile Test (OHTT) and Scanning Electron Microscope (SEM).

## 5.1 Machining conditions for CFRPC

### 5.1.1 Laser machine

Laser machine used in this project is Amada brand with LC.FT NT series and is made in Japan. [35] [36]

Machining conditions for cutting the CFRPC samples by $CO_2$ Laser are provided in Table 5.1.

Table 5.1: $CO_2$ Laser machine conditions

| | | | |
|---|---|---|---|
| **Laser power** | 1000 W | **Lenz** | 5 inch |
| **Frequency** | 1500 HZ | **Nozzle diameter** | 2 mm |
| **Cutting speed** | 2000 mm/min | **Air pressure** | 3bar |
| **Assist gas** | Air | **Gap** (between nozzle and surface) | 1mm |
| **Focal length** | 10.5 mm | **Duty** | 50 |

### 5.1.2 Water-jet machine

Water-jet machine used in this project is Bohler brand and is made in Germany. Machining conditions for cutting the CFRPC samples by Water-jet are provided in Table 5.2.

Table 5.2: Bohler Water-jet machine conditions

| **Water pressure** | **Abrasive substance** |
|---|---|
| 4000 bar | Garnet powder |
| **Flow** | |
| **Initial start** | **Average** |
| 135 Ampere | 35-45mpere |

## 5.2 Machining conditions for GFRP

### 5.2.1 Laser machine

As CFRPC materials are more strength and robust than GFRP, more power must be use for machining. We can also see from Table 4.1 that 1000 (W) has been used for CFRPC. So for making the GFRP samples, 70 (W) is enough.

If we use more power than 70 (W) on GFRPs they will easily melt. However there are some damages after machining even with this power which will be explained later. [35]

It should be noted that different machine powers have been tested on the materials and the best quality in the microscopic view has been chose.

### 5.2.2 Water-jet machine

Conditions of machining on GFRP are similar to CFRPC which is already mentioned on Table 4.2.

## 5.3 Tests

After machining, effects of Laser and Water-jet machines on samples should be studieded by two different sorts of test. Since the purpose of the tests were to measure the strength and quality surface of the materials after machining, Open Hole Tensile Test (OHTT) has been adopted to evaluate thr strength of the samples and furthermore Scanning Electron Microscope (SEM) has been adopted to evaluate the quality surface of the three spots on the machined surface samples.

In this section we discuss what happened during the tests.

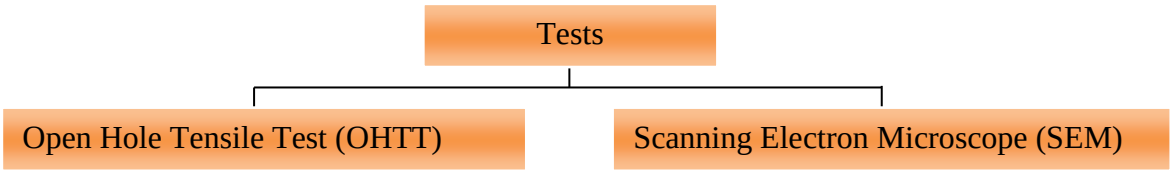


Figure 5.3: Different tests applied on samples

### 5.3.1 Open Hole Tensile Test (OHTT)

As previously discussed samples should have standard dimensions. Then we put the samples in the tensile machine to take the test.

Tensile machine used in this test is INSTRON 4208 made in Britain with capacity of 300 (KN). It must be mentioned that this machine is connected to a server to evaluate diagrams and concludes the output simultaneously, quickly and accurately. It is also important to note that the machine is surely calibrated.

Figure 5.4: Tensile machine

Before taking the test, samples need to be ready. In the gripping areas we must use other materials to avoid failure during the test. According to the type of materials which are polymers, the surfaces are slippery and it can result samples separation from clamps during the test. Wood would be a good choice to intercept these kinds of errors. The resin which has been used to attach the woods to the samples on the gripping area is more viscous than resin which has been used on the samples. Figure 5.5 demonstrates the samples ready for tensile test.

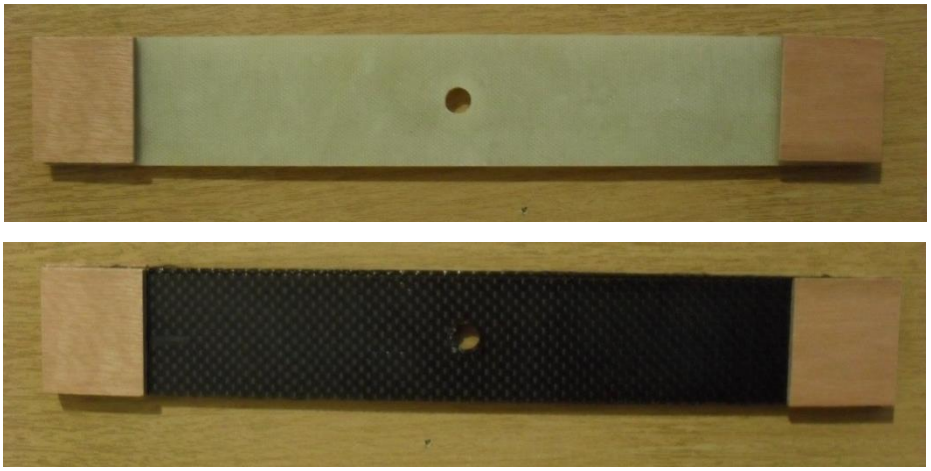

Figure 5.5: Ready samples for tensile test

When prepared samples are fixed in the tensile machine the machine will start working. Meanwhile server records all the conditions including stress-strain curve diagram, ultimate strength and etc. When samples reach to fracture level, the machine work is done and the server will show the outputs.

#### 5.3.1.1 GFRP samples after OHTT

Reaching the fracture point the outputs for GFRP samples will be reviewed. Figure 5.6 and 5.7 depicts GFRP samples at fraction point, machined by Laser and Water-jet machines.

Figure 5.6: Fracture point after Laser machining

Figure 5.7: Fracture point after Water-jet machining

In this section the mechanical properties of GFRP machined samples are presented.

#### 5.3.1.1.1 Sample of GFRP under Water-jet machining by OHTT

Table 4.3 shows the mechanical properties of the GFRP sample under Water-jet machining achieved by OHTT:

Table 5.3: Mechanical properties of GFRP sample under Water-jet machining

| Thickness*width<br>A*b<br>(mm*mm) | Cross section<br>$S_0$<br>($mm^2$) | Ultimate strength<br>$R_m$<br>(MPa) |
|---|---|---|
| 37.84*1.92 | 72.65 | 124 |

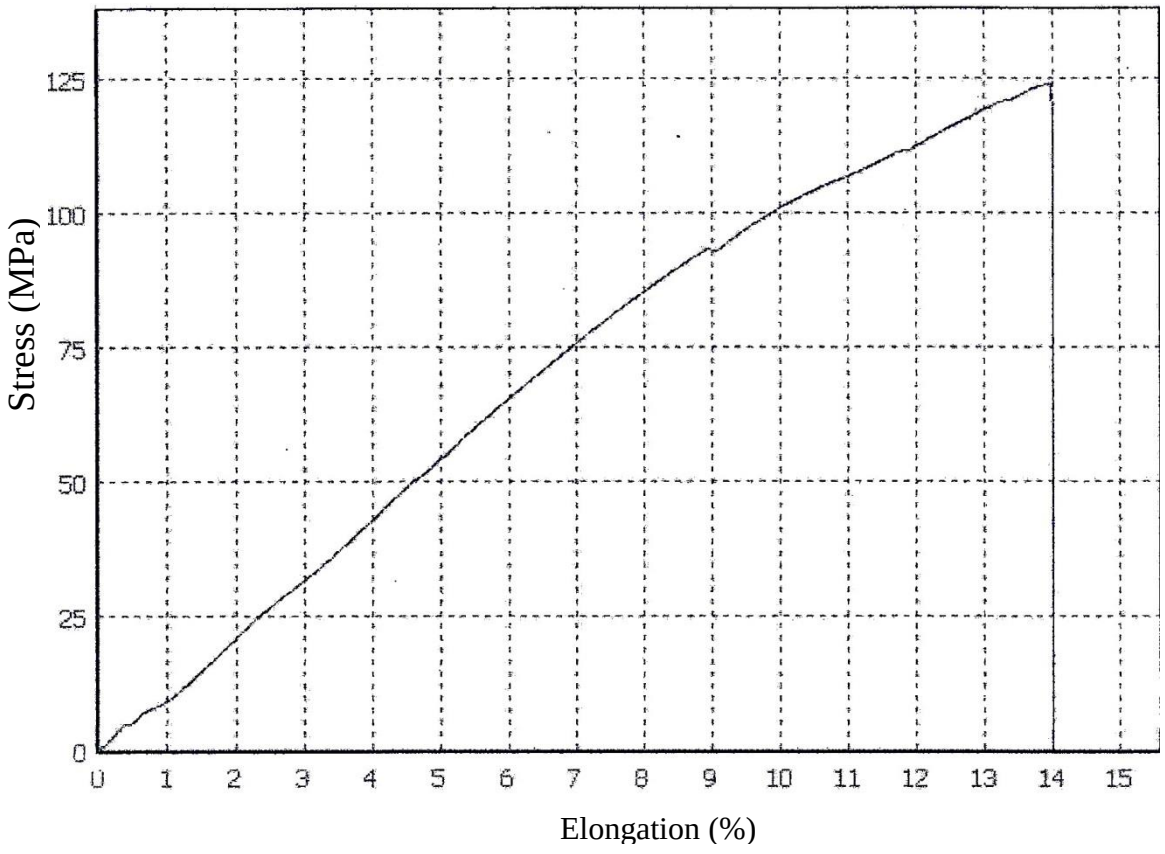


Figure 5.8: Stress-strain curve diagram of the GFRP sample under Water-jet machining by OHTT

#### 5.3.1.1.2 Sample of GFRP under Laser machining by OHTT:

Table 4.4 shows the mechanical properties of the GFRP sample under Laser machining achieved by OHTT.

Table 5.4: Mechanical properties of GFRP sample under Laser machining

| Thickness*width<br>A*b<br>(mm*mm) | Cross section<br>$S_0$<br>($mm^2$) | Ultimate strength<br>$R_m$<br>(MPa) |
|---|---|---|
| 36.84*1.86 | 68.52 | 83 |

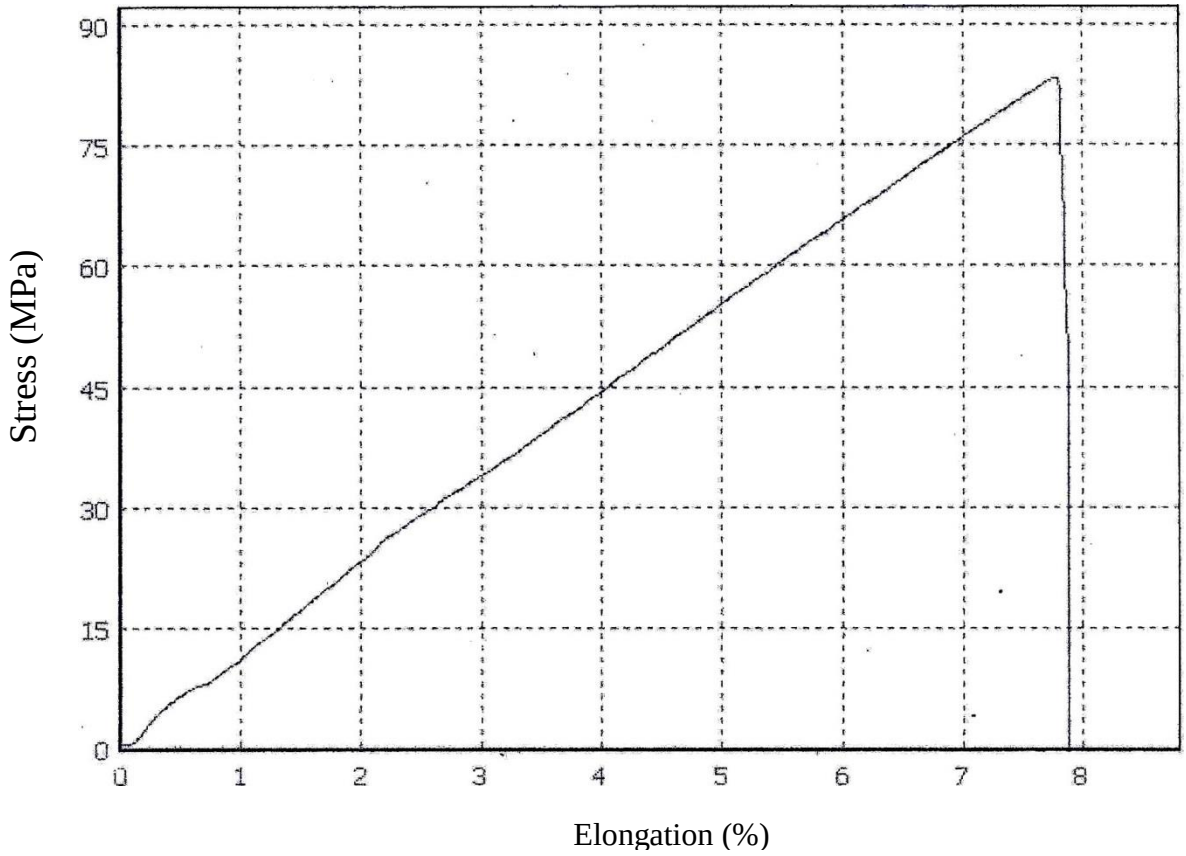


Figure 5.9: The stress-strain curve diagram of the GFRP sample under Laser machining by OHTT

#### 5.3.1.2 CFRPC samples after OHTT

Reaching fracture point the outputs for CFRPC samples will be reviewed. Figure 5.10 and 5.11 depict CFRPC samples machined by Laser and Water-jet machines.

Figure 5.10: Fracture point after Laser machining

Figure 5.11: Fracture point after Water-jet machining

In this section the mechanical properties of CFRPC machined samples are presented.

#### 5.3.1.2.1 Sample of CFRPC under Water-jet machining by OHTT:

Table 5.5 shows mechanical properties of the CFRPC sample under Water-jet machining achived by OHTT.

Table 5.5: Mechanical properties of CFRPC sample under Water-jet machining

| Thickness*width<br>A*b<br>(mm*mm) | Cross section<br>$S_0$<br>($mm^2$) | Ultimate strength<br>$R_m$<br>(MPa) |
|---|---|---|
| 37.96*1.40 | 53.14 | 279 |

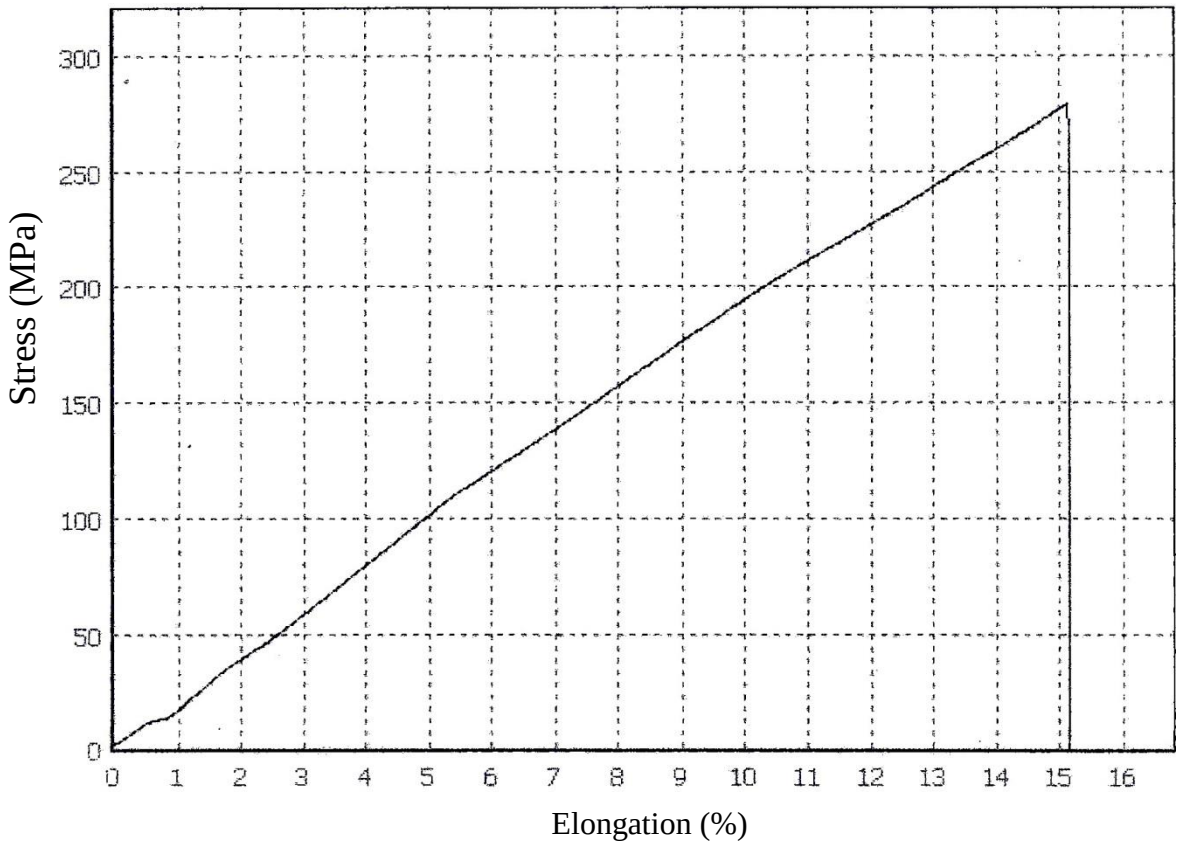


Figure 5.12: Stress-strain curve diagram of the sample Sample of CFRPC from Water-jet machine for OHTT

#### 5.3.1.2.2 Sample of CFRPC under Laser machining by OHTT:

Table 5.6 shows mechanical properties CFRPC sample under Laser machining by OHTT.

Table 5.6: Mechanical properties of CFRPC sample under Laser Machining

| Thickness*width<br>A*b<br>(mm*mm) | Cross section<br>$S_0$<br>($mm^2$) | Ultimate strength<br>$R_m$<br>(MPa) |
|---|---|---|
| 37.18*1.41 | 52.42 | 279 |

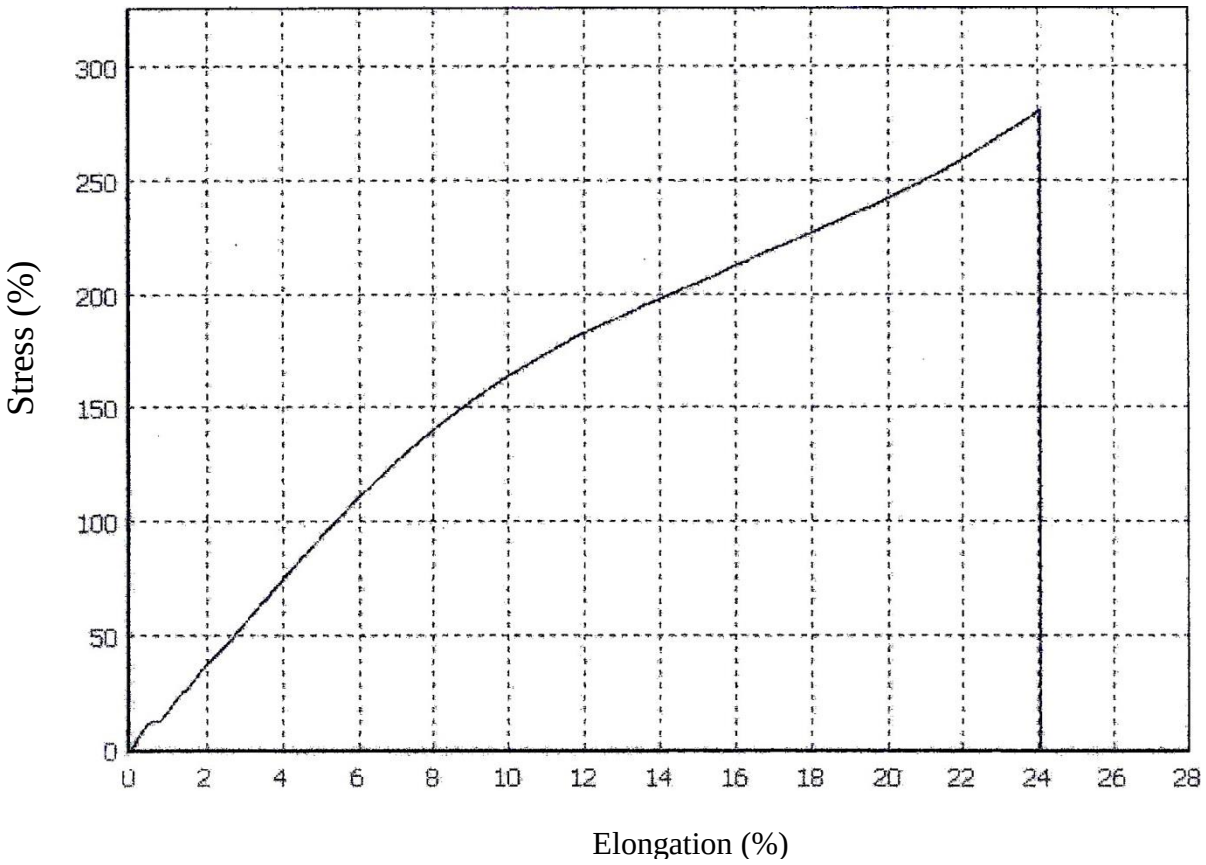


Figure 5.13: Stress-strain curve diagram of the Sample of CFRPC from Laser machine for OHTT

### 5.3.2 Scanning Electron Microscope test (SEM)

TESCAN device, VEGA II model, made in Czech, is the device used on this test.


Figure 5.14: TESCAN microscope

Samples need to be prepared before the test. As the machining samples have 250 millimeter of length, and also because the device has the maximum length of 130 millimeters, samples must reach to 130 millimeter length to fix on the fixture of device. To provide this condition, cutting must be done on the samples. Another preparation of the test names gold coat which is so expensive. A golden coverage on samples is reuired to transmit the electrons on the surface of samples which will provide a better and closer test results.

As illustrated in Figure 5.15 for each sample two areas have been photographed by the microscope.

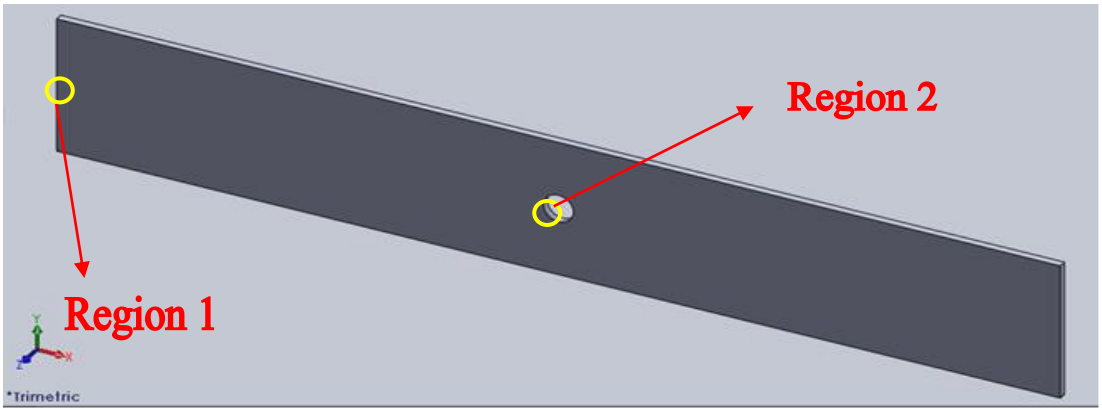


Figure 5.15: Spots for microscope photography

### 5.3.2.1 The GFRP samples after Machining observed by SEM

In this section machined GFRP samples observed by SEM are presented.

#### 5.3.2.1.1 Sample of GFRP under Water-jet machining

Figure 5.16 illustrates the GFRP sample under Water-jet machining observed by SEM.

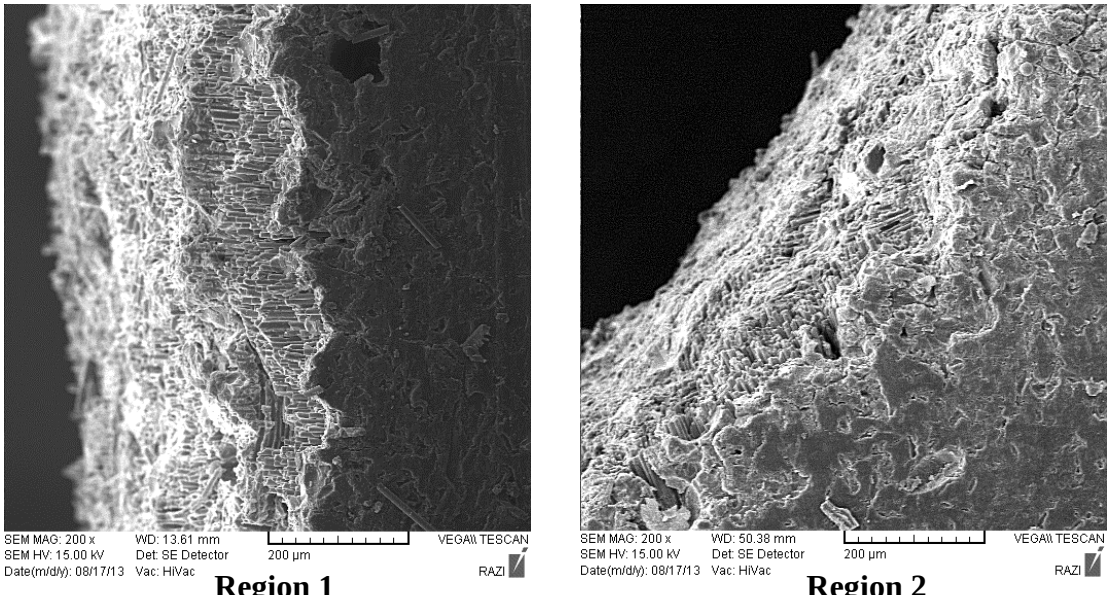


**Region 1** **Region 2**

Figure 5.16: SEM picture of GFRP sample under Water-jet machining with 2mm thichness

#### 5.3.2.1.2 Sample of GFRP under Laser machining

Figure 5.18 illustrates the GFRP sample under Laser machining observed by SEM.

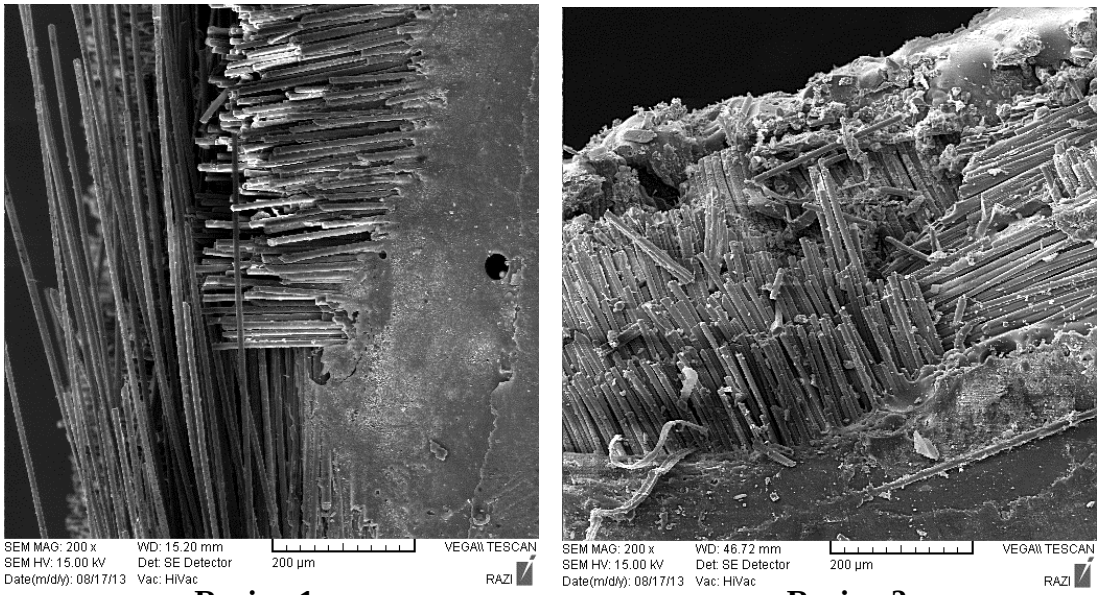


**Region 1** **Region 2**

Figure 5.17: SEM picture of GFRP samples under Laser machining with 2mm thichness

### 5.3.2.2 The CFRPC samples after Machining observed by SEM

In this section machined CFRPC samples observed by SEM are presented.

#### 5.3.2.2.1 Sample of CFRPC under Water-jet machining

Figure 5.18 illustrates the CFRPC sample under Water-jet machining observed by SEM.

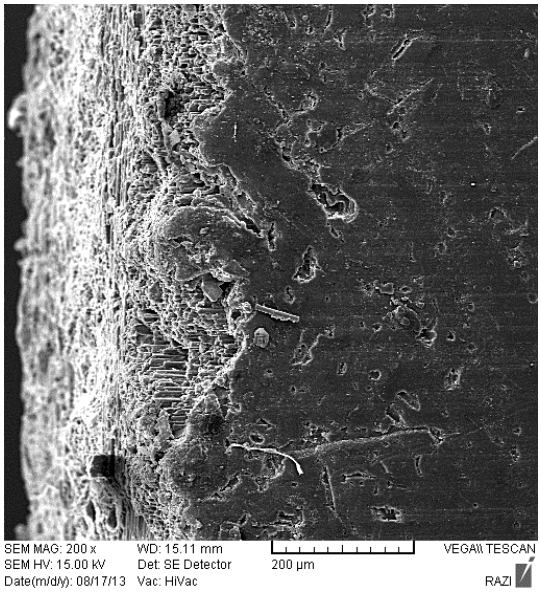


Region 1

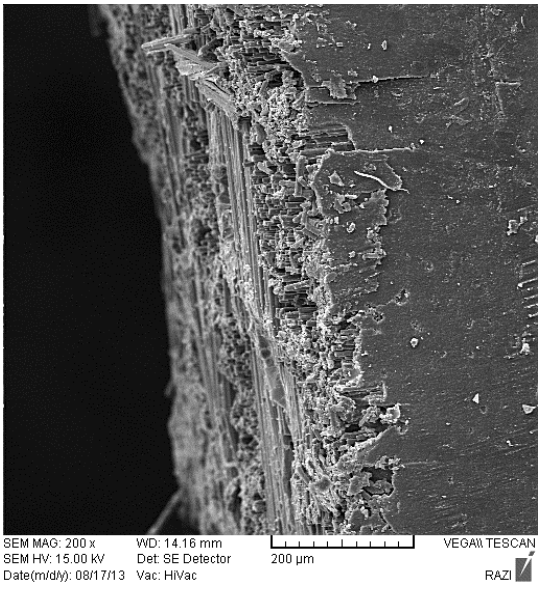


Region 2

Figure 5.18: SEM picture for CFRPC samples under Water-jet machining with 2mm thichness

#### 5.3.2.2.2 Sample of CFRPC under Laser machining

Figure 5.19 illustrates the CFRPC sample under Laser machining observed by SEM.

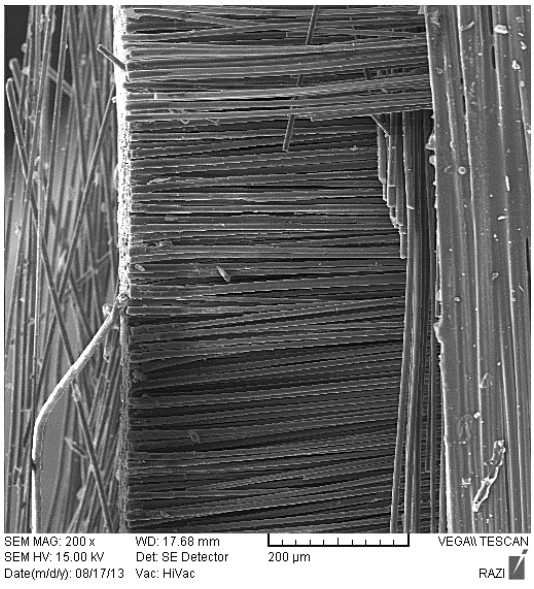


Region 1

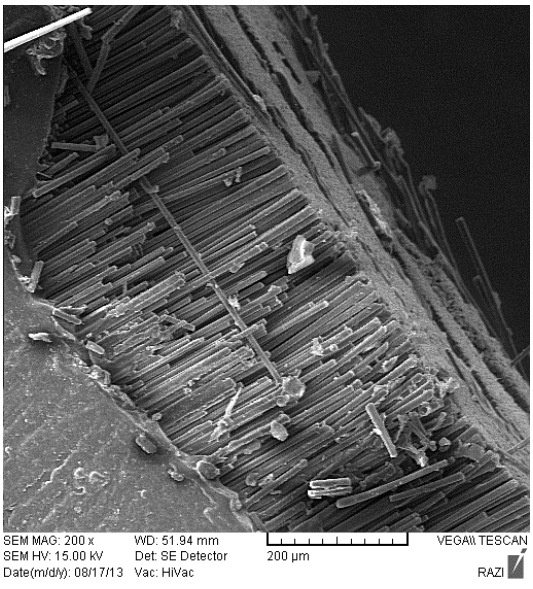


Region 2

Figure 5.19: SEM picture for Sample of CFRPC under Laser machining with 2mm thickness

# Chapter 6

# RESULTS AND DISCUSSION

## 6.1 Surface finish

According to the microscopic part of the experiment and the thesis topic which targets to compare Laser and Water-jet machining, this chapter provides a differential analysis of results based on SEM pictures.

Figure 6.1 depicts different factors to analyze.

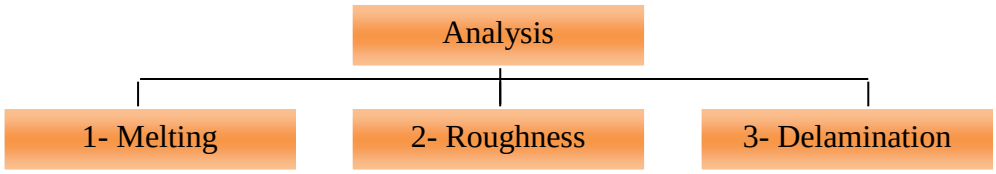


Figure 6.1: Analysis Factors of SEM Pictures

### 6.1.1 Defining the colored lines

To simplify the analysis on the pictures, three colored lines are used for each of the three damages.

- Red line represents the delamination
- Yellow line shows the melting
- Blue line defines the roughness

### 6.1.2 Comparison between Water-jet and Laser machining on GFRP

Figure 6.1 compares the SEM photo of GFRP sample under Laser and Water-jet machining in region 1.

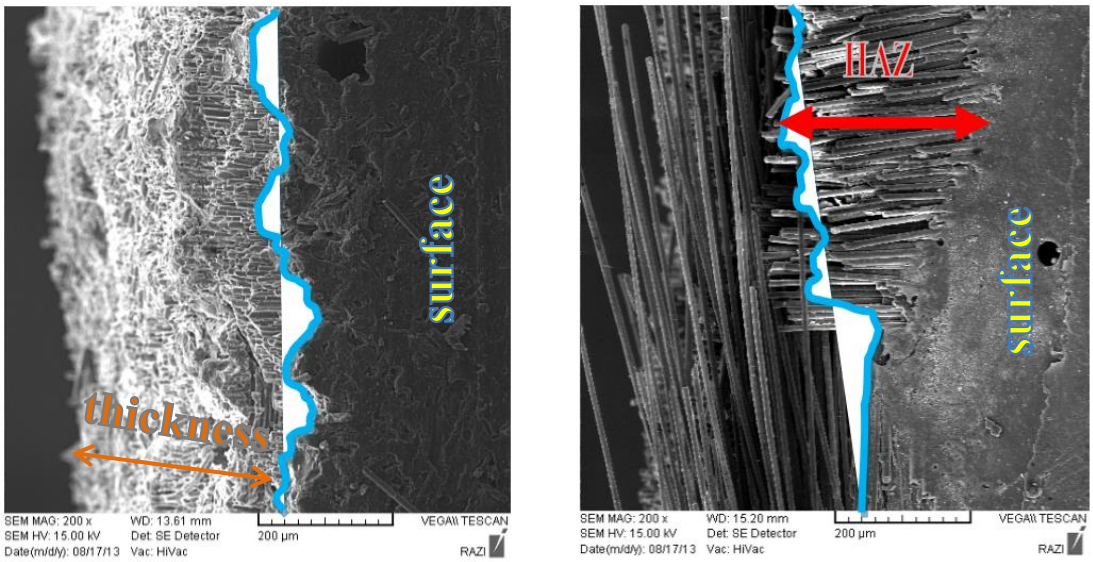


a) b)

Figure 6.2: a) SEM picture of GFRP sample machine by Water-jet
b) SEM picture of GFRP sample machines by Laser

According to Figure 6.1.b the GFRP sample machined by Laser, has too delamination damage to specify the roughness. As demonstrated in Figure 6.1.b the Laser machining process produces a Heat affect zone (HAZ). Absence of melting in this figure is for the reason of using 70 W machine power on the sample due to the GFRP material specifications.

On the other hand as illustrated in Figure 6.1.a the GFRP sample machined by Water-jet, has no delamination therefore there is only the possibility of demonstrating the roughness of the machined area.

Figure 6.2 compares the SEM photo of GFRP sample under Laser and Water-jet machining in region 2.

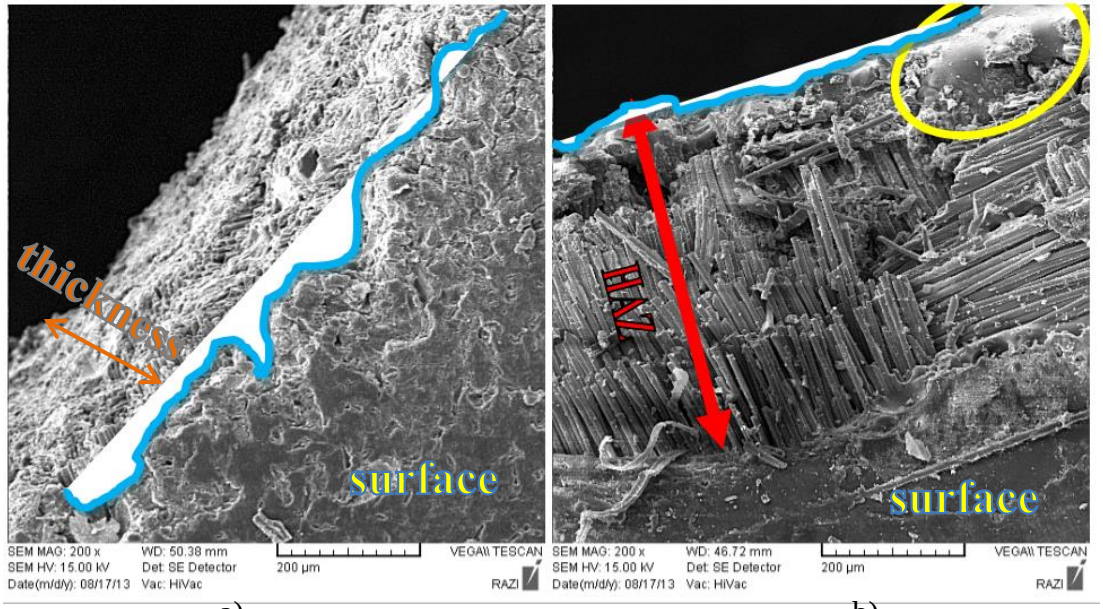


a) b)

Figure 6.3: a) SEM picture of GFRP sample machine by Water-jet
b) SEM picture of GFRP sample machines by Laser

In one hand according to Figure 6.2.a the GFRP sample which has been machined by Laser, has all the three sorts of damages in this area. The cause of melting around the circle is that the thermal effect during the machining process has been too long which means that even if the optic of Laser machine were on the other side of the hole, the heat would still affecting the yellow zone.

On the other hand the GFRP sample which has been machined by Water-jet as depicted in Figure 6.2.a only has the roughness of the machining on the cutting area.

### 6.1.3 Comparison between Water-jet and Laser machining on CFRPC

Figure 6.3 compares the SEM photo of CFRPC sample under Laser and Water-jet machining in region 1.

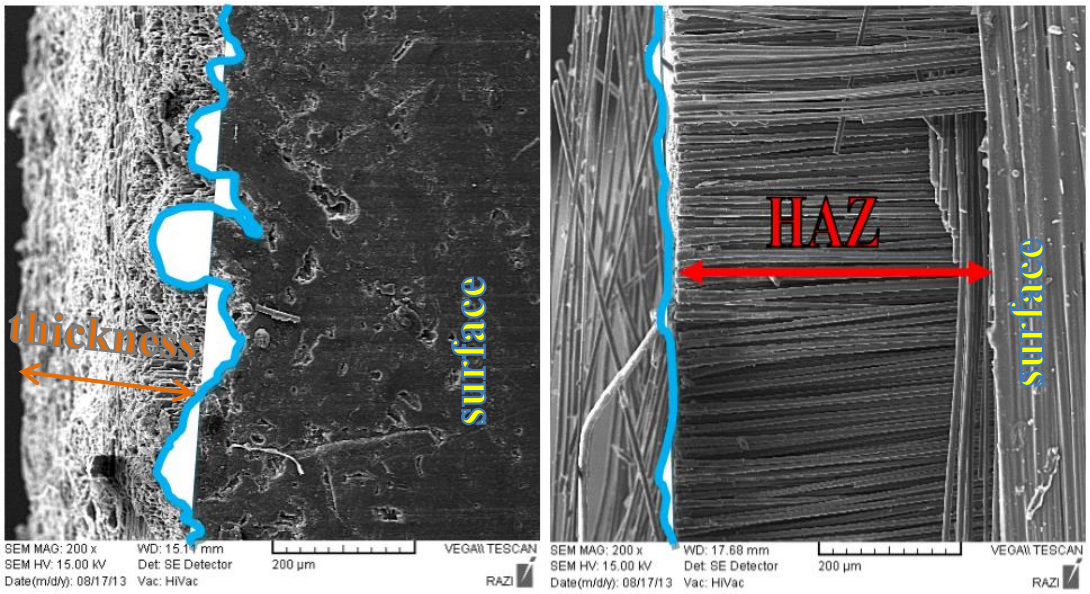


a) b)

Figure 6.4: a) SEM picture for sample of CFRPC from Water-jet machine
b) SEM picture for sample of CFRPC from Laser machine

In Figure 6.3.b the CFRPC sample which has been machined by Laser has been cut well, however there exist some delamination in the cutting area because of the thermal effects of the Laser machine.

In the CFRPC sample which has been machined by Water-jet (left figure), only has roughness in the machining area.

Figure 6.4 compares the SEM photo of CFRPC sample under Laser and Water-jet machining in region 2.

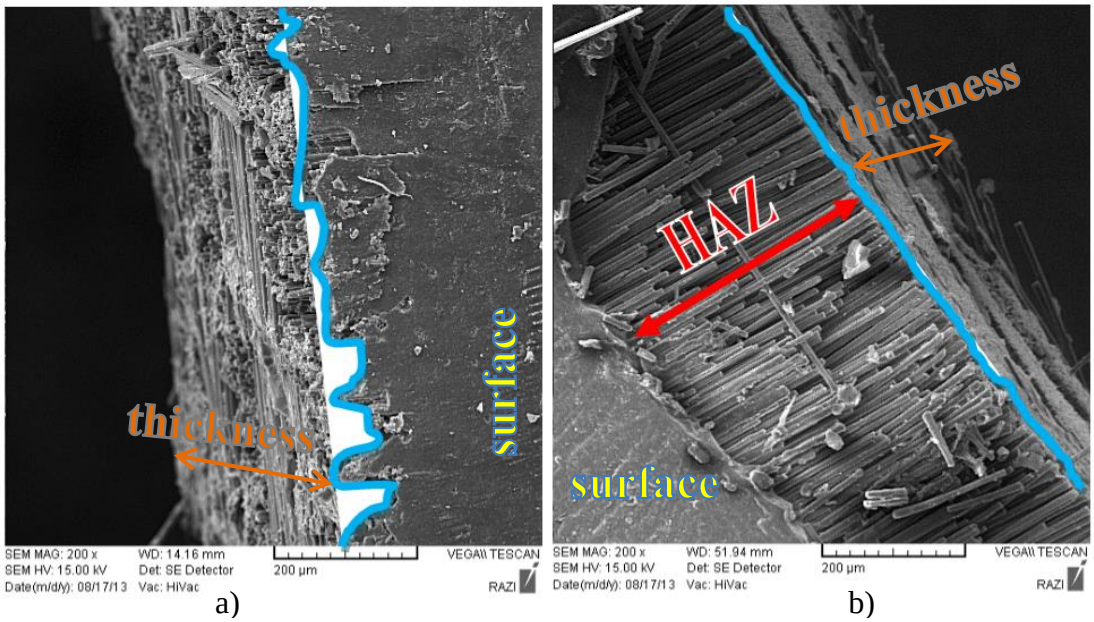


Figure 6.5: a) SEM picture for sample of CFRPC from Water-jet machine
b) SEM picture for sample of CFRPC from Laser machine

As illustrated in Figure 6.4.b the CFRPC sample which has been machined by Laser, has a very low range of roughness which can be neglected, however the delamination is clearly recognizable. On the other hand the only damage appeared on Figure 6.4.a [1] is the roughness.

## 6.2 Calculation of roughness

In this project, roughness is calculated from both Clemex and Excel software combine together. Roughness component indicates the surface quality. Many different roughness parameters have been introduced in the literature but $R_a$ and $R_z$ are two of the most common ones which are studied in this work.

$R_a$ representes the arithmetic mean surface roughness which is calculated as the arithmetical mean of the sums of all profile values.

$R_z$ represents the surface roughness depth which can be calculated as the mean value of the five $R_z$I values from the five sampling length over the total measured length. Equation 6.1 describes $R_z$ where y is the roughness height and n is the number of heights.

$$Rz = \frac{y_1 + y_2 + y_3 + y_4 + ... + y_n}{n} \tag{6.1}$$

In this section we represent diagrams describing roughness parameters $R_a$ and $R_z$. Red dots demonstrate the means of highest heights ($R_z$).

### 6.2.1 Region 1 of GFRP material with Water-jet machine

The diagram in Figure 6.6 demonstrates the roughness in region 1 of GFRP sample machined by Water-jet.

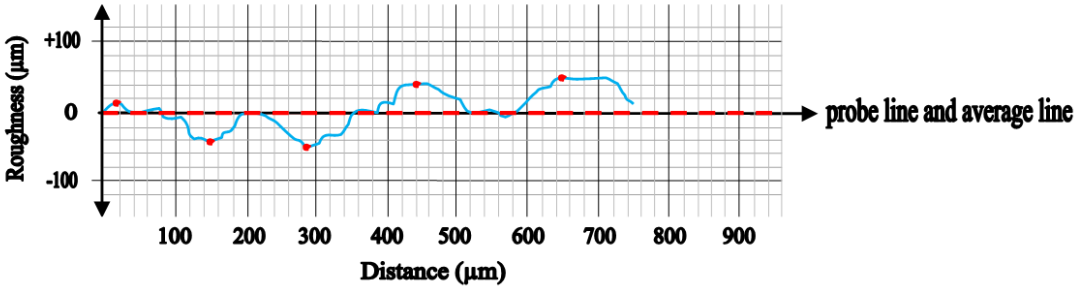


Figure 6.6: Roughness diagram of GFRP with waterjet machining in region 1

The obtained heights to calculate $R_a$ of the mentioned sample are provided in Table 6.1.

Table 6.1: Heights to determine $R_a$ in GFRP sample machined by Water-jet

| | | | | | | | | |
|---|---|---|---|---|---|---|---|---|
| 0 | 0 | 0 | -40 | +20 | +20 | +20 | +40 | Ra |
| +20 | -20 | 0 | -50 | +40 | 0 | +40 | +40 | 2.97 µm |
| 0 | -40 | -20 | -20 | +40 | 0 | +40 | +20 | |
| 0 | -40 | -40 | 0 | +40 | 0 | +40 | | |
| 0 | -20 | -60 | 0 | +20 | 0 | +40 | | |

Table 6.2 contains the five highest heights to estimate $R_z$ in GFRP sample machined by Water-jet.

Table 6.2: Heights to determine $R_z$ in GFRP sample machined by Water-jet

| | $Y_1$ | $Y_2$ | $Y_3$ | $Y_4$ | $Y_5$ | Rz |
|---|---|---|---|---|---|---|
| **Height (µm)** | **20** | **40** | **60** | **60** | **40** | **44** |

### 6.2.2 Region 1 of GFRP material with Laser machine

Figure 6.7 illustrates the roughness diagram in region 1 of GFRP sample under Laser machining.

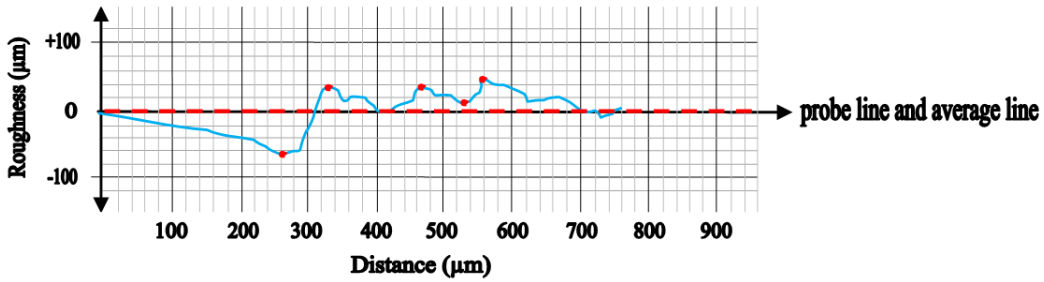


Figure 6.7: Roughness diagram of GFRP with Laser machining in region 1

The diagram of GFRP with both machining shows that the Ra of Laser machine is less than waterjet but we consider both of them zero because the unit for each picture of SEM is 20 µm and the numbers should be rounded. The Rz of Laser machine is less than waterjet.

Table 6.3 provides heights to compute the average roughness in region 1 of GFRP sample machined by Laser.

Table 6.3: Heights to determine $R_a$ in GFRP sample machined by Laser in region 1

| | | | | | | | | |
|---|---|---|---|---|---|---|---|---|
| 0 | -20 | -40 | 40 | 0 | 20 | 20 | 0 | Ra |
| 0 | -20 | -60 | 40 | 20 | 20 | 20 | 0 | |
| 0 | -40 | -60 | 20 | 40 | 40 | 20 | 0 | 0.52 µm |
| -20 | -40 | -60 | 20 | 20 | 40 | 20 | | |
| -20 | -40 | -20 | 0 | 20 | 40 | 0 | | |

The five highest heights to estimate $R_z$ in region 1 of GFRP sample under Laser machining are presented in Table 6.4.

Table 6.4: Heights to determine $R_z$ in region 1 of GFRP sample machined by Laser

| | $Y_1$ | $Y_2$ | $Y_3$ | $Y_4$ | $Y_5$ | $R_z$ |
|---|---|---|---|---|---|---|
| Height (µm) | 60 | 40 | 40 | 20 | 40 | 40 |

### 6.2.3 Region 2 of GFRP with Water-jet machine

Figure 6.8 provides the diagram of roughness in region 2 of GFRP sample with Water-jet machining.

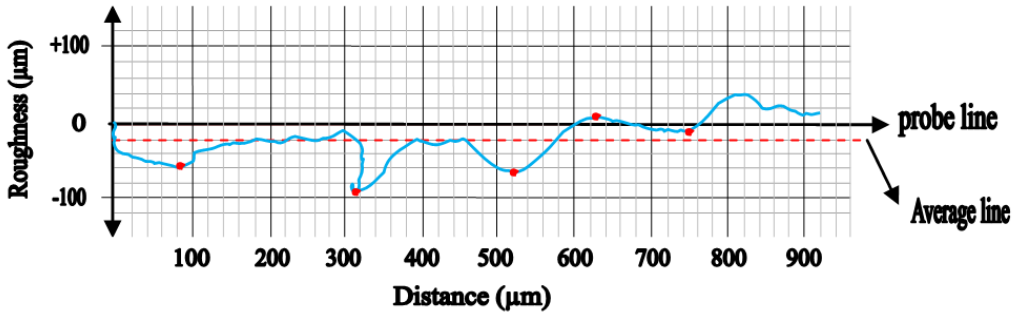


Figure 6.8: Roughness diagram of GFRP with Water-jet machining in region 2

Heights in use to determine the average roughness of GFRP sample in region 2 machined by Water- jet are provided in Table 6.5.

Table 6.5: Heights to determine $R_a$ in GFRP sample machined by Water-jet in region 2

| | | | | | | | | | |
|---|---|---|---|---|---|---|---|---|---|
| 0 | -60 | -20 | -100 | -20 | -60 | 0 | 0 | 40 | Ra |
| -40 | -40 | -20 | -80 | -20 | -60 | 0 | 0 | 40 | 22.66 |
| -60 | -20 | -20 | -60 | -20 | -40 | 0 | 0 | -20 | µm |
| -60 | -20 | -20 | -40 | -40 | -20 | 0 | 20 | -20 | |
| -60 | -20 | 0 | -20 | -60 | 0 | 0 | 40 | -20 | |

Table 6.6 containes the five highest heights to compute $R_z$ in region 2 of GFRP sample machined by Water-jet.

Table 6.6: Heights to determine $R_z$ in GFRP sample machined by Water-jet in region 2

| | $Y_1$ | $Y_2$ | $Y_3$ | $Y_4$ | $Y_5$ | $R_z$ |
|---|---|---|---|---|---|---|
| **Height (µm)** | **60** | **100** | **60** | **20** | **20** | **52** |

### 6.2.4 Region 2 of GFRP material with Laser machine

Figure 6.9 depicts the roughness diagram of GFRP sample with Laser machining in region 2.

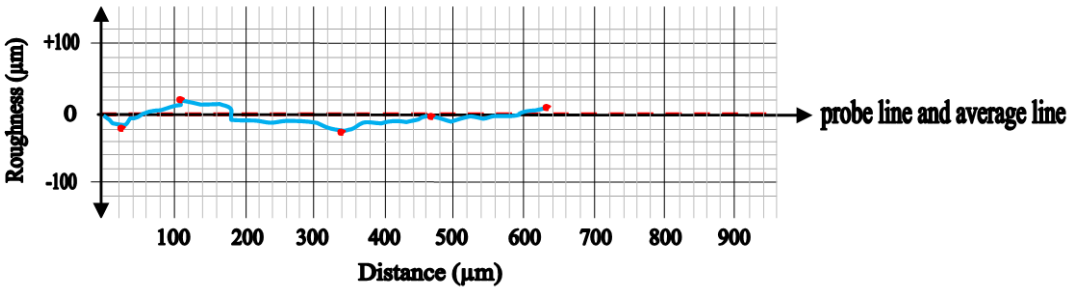


Figure 6.9: Roughness diagram of GFRP with Laser machining in region 2

In region 2 the diagram shows that both Ra and Rz of Laser machine are less than the Water-jet. Table 6.7 containes the heights used to determine the average roughness of GFRP sample by Laser in region 2.

Table 6.7: Heights to determine $R_a$ in GFRP sample machined by Laser in region 2

| | | | | | | | |
|---|---|---|---|---|---|---|---|
| 0 | 20 | 0 | 0 | 0 | 0 | 0 | Ra |
| -20 | 20 | 0 | -20 | 0 | 0 | 20 | 0.62 µm |
| 0 | 20 | 0 | -20 | 0 | 0 | | |
| 0 | 20 | 0 | -20 | 0 | 0 | | |
| 0 | 0 | 0 | 0 | 0 | 0 | | |

The five highest heights and the resulted $R_z$ are presented in Table 6.8.

Table 6.8: Heights to determine $R_z$ in GFRP sample machined by Laser in region 2

| | $Y_1$ | $Y_2$ | $Y_3$ | $Y_4$ | $Y_5$ | $R_z$ |
|---|---|---|---|---|---|---|
| **Height (µm)** | **20** | **20** | **20** | **20** | **20** | **20** |

### 6.2.5 Region 1 of CFRPC with Water-jet machine

Figure 6.10 illustrates the surface roughness of CFRP sample with Water-jet machining in region 1.

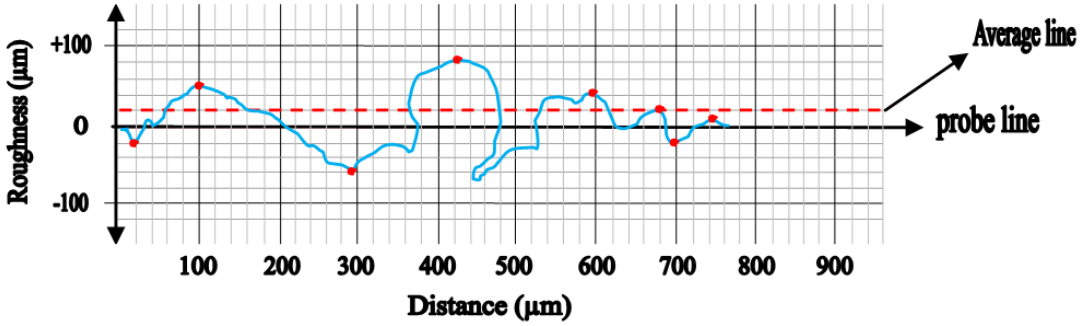


Figure 6.10: Roughness diagram of CFRPC with Water-jet machining in region 1

The average surface roughness is calculated using the heights presented in Table 6.9.

Table 6.9: Heights to determine $R_a$ in CFRPC sample machined by Water-jet

| | | | | | | | | |
|---|---|---|---|---|---|---|---|---|
| 0 | 60 | 0 | -40 | 80 | -20 | 40 | -20 | Ra |
| -20 | 40 | -20 | -40 | 80 | 0 | 0 | 0 | |
| 0 | 40 | -20 | -20 | 80 | 40 | 0 | 20 | 16.31 µm |
| 20 | 20 | -20 | 20 | 80 | 40 | 20 | 0 | |
| 40 | 20 | -40 | 60 | 20 | 40 | 20 | | |

Table 6.10 contains the five highest heights to calculate the parameter $R_z$.

Table 6.10: Heights to determine $R_z$ in CFRPC sample machined by Water-jet

| | $Y_1$ | $Y_2$ | $Y_3$ | $Y_4$ | $Y_5$ | $R_z$ |
|---|---|---|---|---|---|---|
| **Height (µm)** | **20** | **60** | **60** | **80** | **40** | **52** |

### 6.2.6 Region 1 of CFRPC with Laser machine

Roughness diagram of CFRPC with Laser machining in region 1 is depicted in Figure 6.11.

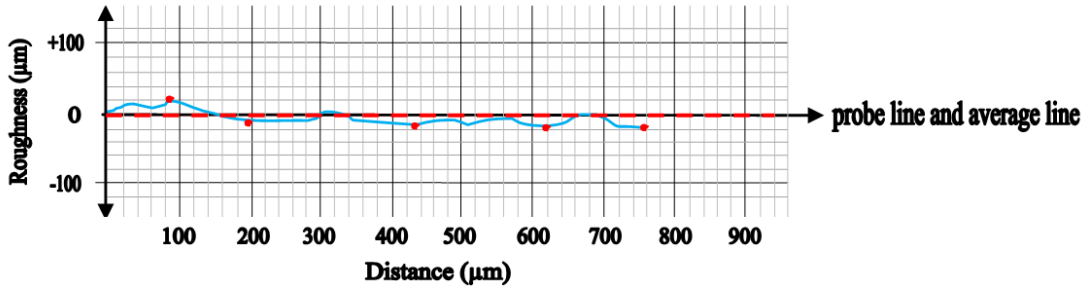


Figure 6.11: Roughness diagram of CFRPC with Laser machining in region 1

It has been observed that in CFRPC the Ra and Rz parameters of Laser machine are less than waterjet machine. Table 6.11 provides the heights to determine the parameter $R_a$ in region 1 of CFRPC sample machined by Laser.

Table 6.11: Heights to determine $R_a$ in CFRPC sample machined by Laser in region 1

| | | | | | | | |
|---|---|---|---|---|---|---|---|
| 0 | 0 | -20 | -20 | 0 | -20 | 0 | Ra |
| 0 | 0 | 0 | -20 | -20 | -20 | -20 | 7.05 µm |
| 0 | 0 | 0 | -20 | 0 | -20 | -20 | |
| 0 | 0 | -20 | 0 | 0 | 0 | -20 | |
| +20 | 0 | -20 | 0 | 0 | 0 | | |

Selected heights to estimate the $R_z$ are presented in Table 6.12.

Table 6.12: Heights to determine $R_z$ in CFRPC sample machined by Laser

| | $Y_1$ | $Y_2$ | $Y_3$ | $Y_4$ | $Y_5$ | $R_z$ |
|---|---|---|---|---|---|---|
| **Height (µm)** | **20** | **20** | **20** | **20** | **20** | **20** |

### 6.2.7 Region 2 of CFRPC with Water-jet machine

Figure 6.12 demonstrates the roughness diagram of region 2 of CFRPC with Water-jet machining.

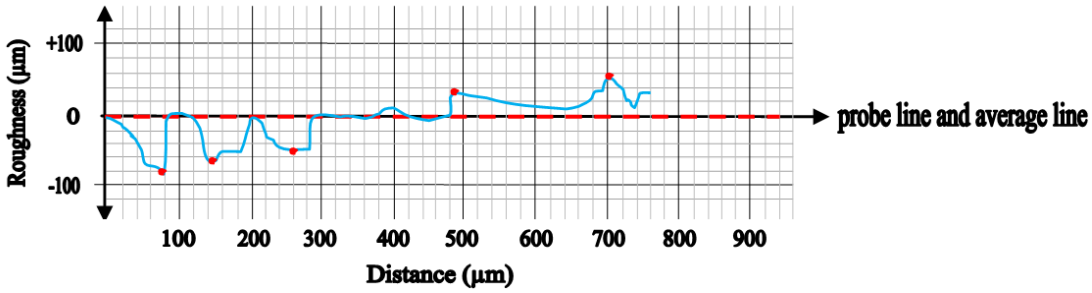

Figure 6.12: Roughness diagram of CFRPC with Water-jet machining in region 2

Heights to determine $R_a$ in CFRPC sample machined by Water-jet in region 2 are provided in Table 6.13.

Table 6.13: Heights to determine $R_a$ in CFRPC sample machined by Water-jet in region 2

| | | | | | | | | |
|---|---|---|---|---|---|---|---|---|
| 0 | 0 | 0 | 0 | 0 | 20 | 20 | 60 | Ra |
| -20 | 0 | -20 | 0 | 0 | 20 | 0 | 40 | 7.17 µm |
| -40 | -60 | -40 | 0 | 0 | 20 | 0 | 0 | |
| -80 | -60 | -60 | 0 | 0 | 20 | 20 | 40 | |
| -80 | -60 | -60 | 0 | 0 | 20 | 20 | | |

The five highest heights resulting the parameter $R_z$ are provided in Table 6.14.

Table 6.14: Heights to determine $R_z$ in CFRPC sample machined by Water-jet in region 2

| | $Y_1$ | $Y_2$ | $Y_3$ | $Y_4$ | $Y_5$ | $R_z$ |
|---|---|---|---|---|---|---|
| **Height (µm)** | **80** | **60** | **40** | **20** | **40** | **48** |

### 6.2.8 Region 2 of CFRPC with Laser machine

The roughness diagram of CFRPC with Laser machining in region 2 is illustrated in Figure 6.13.

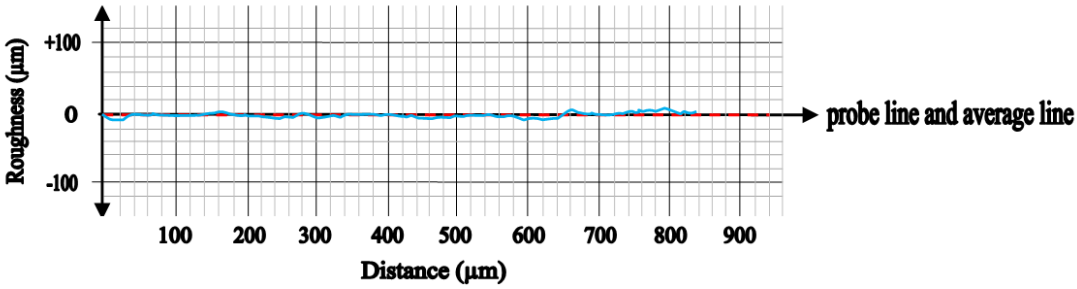


Figure 6.13: Roughness diagram of CFRPC with Laser machining in region 2

It has been concluded that in region 2 of CFRPC the Ra and Rz parameters of Laser machine is less than waterjet. Table 6.15 presents the heights to estimate the average roughness in region 2 of CFRPC machined by Laser.

Table 6.15: Heights to determine $R_a$ in CFRPC sample machined by Laser in region 2

| | | | | | | | | | |
|---|---|---|---|---|---|---|---|---|---|
| 0 | 0 | 0 | 0 | 0 | 0 | 0 | 0 | 0 | Ra |
| 0 | 0 | 0 | 0 | 0 | 0 | 0 | 0 | 0 | 0 |
| 0 | 0 | 0 | 0 | 0 | 0 | 0 | 0 | | µm |
| 0 | 0 | 0 | 0 | 0 | 0 | 0 | 0 | | |
| 0 | 0 | 0 | 0 | 0 | 0 | 0 | 0 | | |

Table 6.16 contains the five selected highest heights used to calculate the $R_z$.

Table 6.16: Heights to determine $R_z$ in CFRPC sample machined by Laser in region 2

| $R_z$ | $Y_1$ | $Y_2$ | $Y_3$ | $Y_4$ |
|---|---|---|---|---|
| **Height (µm)** | **0** | **0** | **0** | **0** |

As the roughness curve in Figure 6.13 nearly tangents to the horizontal axis all the selected heights , $R_a$ and $R_z$ are considered zero.

## 6.3 Comparison between the tensile strength of the materials after machining

After machining the CFRPC and GFRP materials, samples evaluated by the Open Hole Tensile Test have been discussed in the Experimental phase. In this section the the graphs and data obtained from the test will be compared and subsequently the two kinds of machining will be analysed.

### 6.3.1 Tensile strength between the Laser and Water-jet machining on GFRP

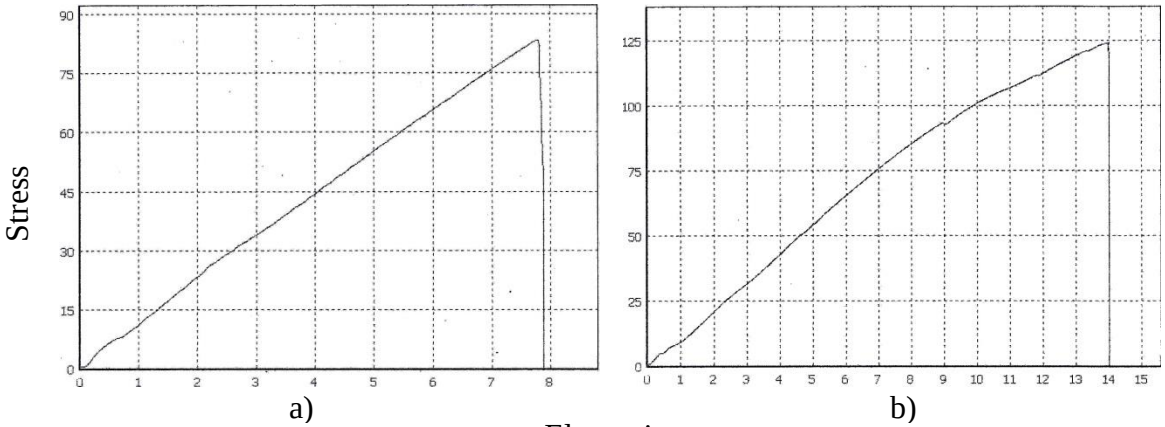


Figure 6.14: a) OHTT sample for GFRP from Laser machining
b) OHTT sample for GFRP from Water-jet machining

As Figure 6.12.a shows, the GFRP sample machined by Laser has a significant difference in ultimate strength tcompared to the GFRP sample machined by Water-jet which is illustratd in Figure 6.12.b. The ultimate strength of Water-jet sample is 124 (MPa), while the ultimate strength of Laser sample is 83MPa.

In both graphs, the ultimate tensile strength is exactly fracture point. This means that both materials have not been necking so they do not have an elastic region and finally both materials are brittle. But the GFRP sample which has been machined by Water-jet has a highest strength after machining because of the surface quality.

### 6.3.2 Tensile strength between Laser and Water-jet machining on CFRPC composite

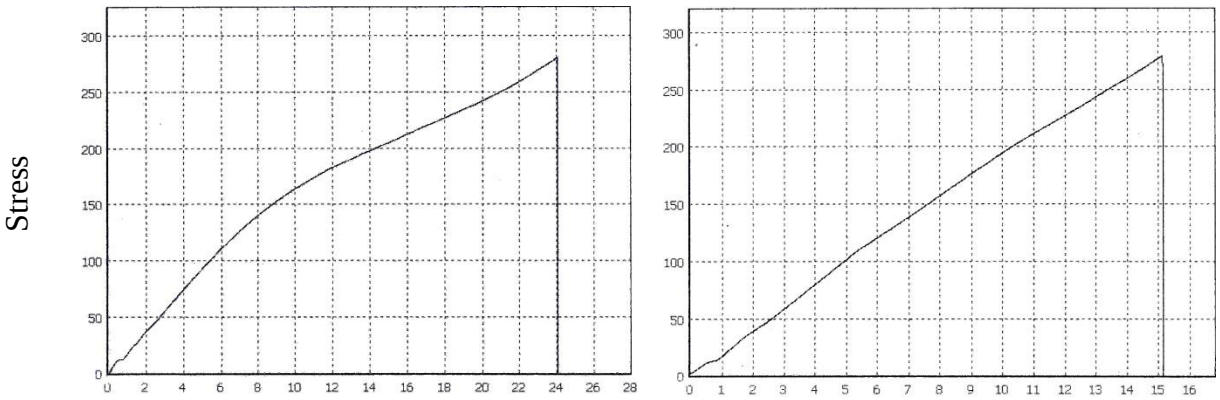


Figure 6.15: a) OHTT sample for CFRPC from Laser machining
b) OHTT sample for CFRPC from Water-jet machining

As depicted in Figure 6.13 the ultimate strength of the CFRPC samples which has been machined by Laser (Figure 6.13.a) and Water-jet (Figure 6.13.b) are both equal which is very interesting. The ultimate strength in both cases was equal to 279 MPa.

## 6.4 Surface quality, time and costs

### 6.4.1 Surface quality

For the surface quality we have represented three indexes namely: roughness, melting and delamination. For each index the points of penalty have been assigned from 0 to 2 where the highest point shows the worst situation. After summation of the points, total number shows the surface quality of the sample.

As you can see in Tables 6.17 and 6.18, the range of the penalty points are from 1 to 4. So we categorize the points as following:

1- Very good

2- Good

3- Average

4- Weak

Table 6.17: surface quality pointing for CFRPC

| | **CFRPC** | | | | | |
|---|---|---|---|---|---|---|
| | **Water-jet** | | | **Laser** | | |
| | **roughness** | **melting** | **delamination** | **roughness** | **melting** | **delamination** |
| **0** | | ✓ | ✓ | | ✓ | |
| **1** | | | | ✓ | | |
| **2** | ✓ | | | | | ✓ |
| **total** | **2** | | | **3** | | |

Table 6.18: surface quality pointing for GFRP

| | GFRP | | | | | |
|---|---|---|---|---|---|---|
| | Water-jet | | | Laser | | |
| | roughness | melting | delamination | roughness | melting | delamination |
| 0 | | ✓ | ✓ | | | |
| 1 | | | | ✓ | ✓ | |
| 2 | ✓ | | | | | ✓ |
| total | 2 | | | 4 | | |

### 6.4.2 Timing and costs

Time has been calculated by the technique of stop watch. For more information each plat of materials can accommodate 7 samples. During the machining of each plat by Water-jet and Laser time of the machining has been calculated and the average time of the six samples of one plat is considered as the process time of machining of one sample.

As the speed of the Laser machining has been equal for both GFRP and CFRPC materials and the only thing which was changed for each material was the machine power, the timing was similar and it was equal to 128 seconds per sample. This timing was also about 35 seconds per sample in Water-jet machining for both GFRP and CFRPC materials but the power in this process was also the same and it was equal to 4000 bar pressure.

Costs of Water-jet machining for polymer materials were about 30$ per hours or 0.5$ per minutes. The exact cost of Laser machining was twice more than Water-jet which is equal to 60$ per hour or 0.5$ per second.

Cost per samples has been calculated by equation 6.2 and finally these calculations have been getting together in Table 6.19.

$$\text{cost per sample} = \frac{(\text{Average time of machining one sample(s)} \times \text{cost of machine per time (\$)})}{60\ (\text{s})} \quad (6.2)$$

Table 6.19: Comparison between Surface quality, time and costs

| machine | material | Surface quality | Ultimate strength (MPa) | Time per sample (S) | Cost per sample ($) |
|---|---|---|---|---|---|
| Water-jet | CFRPC | Good | 279 | 35 | 0.29 |
| | GFRP | Good | 124 | 35 | 0.29 |
| Laser | CFRPC | Average | 279 | 128 | 2.13 |
| | GFRP | Weak | 83 | 128 | 2.13 |

# Chapter 7

# CONCLUSION

In this study, the effect of two advnace machining, namely Water-jet and Laser, were investigated on machining of CFRPC and GFRP. The following conclusions are drawn from the study:

1.Melting of ploymer phase is the consequence of thermal effects of Laser machining which has occurred only in the second region (around the hole) of the samples and that is because of greater temperature focus on the small area. Also delamination is another thermal effect, because the heat will destroy the resin of the cutting area and then will cause the delamination around this area.

2.The remarkable point of the project is that not only Water-jet machining has the better surface quality, but also financially it is more affordable than Laser machine.The cost of Laser machining is twice more than Water-jet and further more it wastes more time in comparison to Water-jet.

According to all the points during the experiment and also points below, Water-jet machine is more advantageous than Laser machine.

- More surface quality
- Lower Delamination and no Melting
- Shorter machining time

- Less cost

# REFERENCES


[1] A.K.Bhargava., "Engineering materials polymers," *Ceramic and Composites*, pp. 226-235, 2005.

[2] J. George, D.Shah, R. G. Jivani, D. Gupta., "Abrasive Water-jet," *a review, National Conference on Recent Trends in Engineering & Technology*, 2011.

[3] L.M.P. Durão , M.F.S.F. de Moura , A.T. Marques, "Numerical prediction of delamination onset in carbon/epoxy composites drilling," *Engineering Fracture Mechanics*, pp. 2767–2778, 2008.

[4] S.R. Ravishankar, C.R.L. Murthy, "Characteristics of AE signals obtained during drilling composite laminates," *NDT&E International*, pp. 341-348, 2000.

[5] Edoardo Capello, "Workpiece damping and its effect on delamination damage in drilling thin composite laminates," *Journal of Materials Processing Technology*, vol. 148, pp. 186–195, 2004.

[6] Tagliaferri V., Di Ilio A. , Visconti C., "Laser cutting of fibre-reinforced polyesters," *Composites*, vol. 16, pp. 317–325, 1985.

[7] Caprino G. , Tagliaferri V., "Maximum cutting speed in Laser cutting of fiber," *Int J Mach Tool Manuf*, vol. 28, pp. 389–398, 1988.

[8] Davim JP, Barricas N, Conceiçao M, Oliveira C., "Some experimental studies on CO2 Laser cutting quality of polymeric materials," *J Mater Process Technol*, vol. 198, pp. 99–104, 2008.

[9] Lau WS., Lee WB., Pang SQ., "Pulsed Nd:YAG Laser cutting of carbon fibre composite materials," *Manuf Technol*, vol. 39, pp. 179–82, 1990.

[10] Hocheng H. , Pan CT., "Section area of heat affected zone in Laser cutting of carbon fiber-reinforced PEEK," *Am Soc Mech Eng*, pp. 153–165, 1993.

[11] G. Caprino, V. Tagliaferri and L. Covelli, "The Importance of Material Structure in the Laser Cutting of Glass Fiber Reinforced Plastic Composites," *J. Eng. Mater. Technol*, vol. 117(1), pp. 133-138, 1995.

[12] Al-Sulaiman, FA; Yilbas, BS; Ahsan, M, "CO2 Laser Cutting Of A Carbon/Carbon Multi-Lamelled Plain-Weave Structure," *JOURNAL OF MATERIALS PROCESSING TECHNOLOGY*, vol. 173, pp. 345-351, 2006.

[13] A. A. Cenna, P. Mathew, "Evaluation of cut quality of fibre-reinforced plastics—A review," *International Journal of Machine Tools & Manufacture*, vol. 37(6), pp. 723-736., 1997.

[14] Jose Mathew , G.L. Goswami , N. Ramakrishnan, N.K. Naik, "Parametric studies on pulsed Nd:YAG Laser cutting of carbon fibre reinforced plastic

composites," *Journal of Materials Processing Technology*, vol. 89-90, pp. 198–203, 1999.

[15] Z.L. Li, H.Y. Zheng, G.C. Lim, P.L. Chu, L. Li, "Study on UV Laser machining quality of carbon fibre reinforced composites," *Composites: Part A*, vol. 41, pp. 1403–1408, 2010.

[16] D. Herzog, P. Jaeschke, O. Meier, and H. Haferkamp, "Investigations on the thermal effect caused by Laser cutting with respect to static strength of CFRP," *Tools Manuf.*, vol. 48(12-13), pp. 1464–1473, 2008.

[17] G. Chryssolouris, P. Sheng and N. Anastasia, "Laser Grooving of Composite Materials With the Aid of a Water-jet," *J. Manuf. Sci. Eng.*, vol. 115(1), pp. 62-72, 1993.

[18] Peter Jaeschke, Dirk Herzog, Christian Noelke, Bjoern Henning andHeinz Haferkamp, "Investigations into the Sealing of Heat Damaged Areas by Applying Polymer Powders During Laser Cutting of Carbon Fiber Reinforced Composites," *Advanced Engineering Materials*, vol. 12, no. 7, pp. 587–590, 2010.

[19] F. Quintero, J. Pou, F. Lusquiños, M. Boutinguiza, R. Soto, and M. Pérez-Amor, "Comparative study of the influence of the gas injection system on the Nd:yttrium-aluminum-garnet Laser cutting of advanced oxide ceramics,"

*Review of Scientific Instruments*, vol. 74, pp. 4199-4205, 2003.

[20] Charles L. Caristan, *Laser cutting : guide for manufacturing*. Dearborn, Mich.: SME, Society of Manufacturing Engineers , 2004.

[21] A., Quintero, F., Lusquiños, F., Pou, J., Pérez-Amor, M. Riveiro, "Laser cutting of 2024-T3 aeronautic aluminum alloy," *Journal of Laser Applications*, vol. 20 (4), pp. 230-235, 2008.

[22] Carlos Oliveira, Nuno Barricas, Marta Conceição J. Paulo Davim, "Evaluation of cutting quality of PMMA using CO2 Lasers," *The International Journal of Advanced Manufacturing Technology*, vol. 35, no. Issue 9-10, pp. 875-879, 2008.

[23] Pou, J.& Boutinguiza, M.& Quintero, F.& Lusquiños, F.& Soto, R.& Pérez-Amor, M., "Comparative study of the cutting of car interior trim panels reinforced by natural fibers," *J Laser Appl*, vol. 13, no. 3, pp. 90-95, 2001.

[24] J. Wang, "Abrasive Waterjet Machining of Polymer Matrix Composites," *International Journal of Advanced Machining Technology*, vol. 15, pp. 757-768, 1999.

[25] J. Wang, "Predictive depth of jet penetration models for abrasive waterjet cutting of," *Int. J. of Mechanical Sciences*, vol. 49, pp. 306-316, 2007.

[26] M. Hashish, "Status and potential of waterjet machining of composites," , Huston, Texas, 1999, p. 64.

[27] A.W. Momber,R. Kovacevic, "Principles Of Abrasive Water-jet Machining," *Springer*, 1998.

[28] Mahesh Haldankar, "Experimental and FEA of particle impact erosion for polymer composites," *International Journal of Mechanical and Production*, vol. 1, no. 5, pp. 2320-2092, Nov. 2013.

[29] A Alberdi, "Composite cutting with abrasive Water-jet," in *Proceedings of 5th Manufacturing Engineering Society International Conference*, Zaragoza, June,2013.

[30] E Leema, "Study of Cutting Fiber-Reinforced Composites by Using Abrasive Waterjet with Cutting head Oscillation," *Composite Structures*, vol. 55, pp. 297-303, 2002.

[31] Steven L. Donaldson, Daniel B. Miracle, *ASM Handbook Composites Volume 21*.: ASM International, 2001.

[32] Alexandre Mondelin, Benoit Furet, Joel Rech , "Characterisation of friction properties between a laminated carbon fibres reinforced polymer and a monocrystalline diamond under dry or lubricated conditions," *Tribology*

*International*, vol. 43, pp. 1665–1673, 2010.

[33] E. Brinksmeier, S. Fangmann, R. Rentsch, "Drilling of composites and resulting surface integrity," *CIRP Annals - Manufacturing Technology*, vol. 60, pp. 57-60, 2011.

[34] Vahid Majidi, *Traditional machining of polymer composite*.

[35] (2013, November) [Online]. http://www.amada.co.jp/

[36] (2013, December) [Online]. http://www.powerautomation.de

[37] Giovanni Belingardi, Ermias Gebrekidan Koricho, Alem Tekalign Beyene, "Characterization and damage analysis of notched cross-ply and angle-ply fabric GFRP composite material," *Composite Structures*, pp. 237-249, March 2013.

[38] Claus Dolda, Marcel Henerichsb, Lennart Bochmannb, Konrad Wegenera, "Comparison of ground and Laser machined polycrystalline diamond (PCD) tools in cutting carbon fiber reinforced plastics (CFRP) for aircraft structures," *Procedia CIRP*, pp. 178 – 183, 2012.

[39] C.T. Pan, H. Hocheng, "Evaluation of anisotropic thermal conductivity for unidirectional FRP in Laser machining," *Composites: Part A*, pp. 1657-1667, 2000.

[40] A. Riveiro, F. Quintero, F. Lusquiños, J. del Val, R. Comesaña, M. Boutinguiza, J. Pou, "Experimental study on the CO2 Laser cutting of carbon fiber reinforced plastic composite," *Composites: Part A*, pp. 1400-1409, February 2012.

[41] Dirk Herzog, Peter Jaeschke, Oliver Meier, Heinz Haferkamp, "Investigations on the thermal effect caused by Laser cutting with respect to static strength of CFRP," *International Journal of Machine Tools & Manufacture*, pp. 1464–1473, 2008.

[42] A.N. Fuchs ,M. Schoeberl, J. Tremmer, M.F. Zaeh, "Laser cutting of carbon fiber fabrics," *Physics Procedia*, pp. 365 – 373, 2013.

[43] James C. Williams , Edgar A. Starke, Jr., "Progress in structural materials for aerospace systems," *Acta Materialia 51*, pp. 5775-5799, August 2003.

[44] Johannes Stock , Michael F. Zaeh, Markus Conrad, "Remote Laser Cutting of CFRP: Improvements in the Cut Surface," *Physics Procedia*, pp. 161 – 170, 2012.

[45] E. Uhlmann, G. Spur, H. Hocheng, S. Liebelt, C.T. Pan, "The extent of Laser-induced thermal damage of UD and crossply composite laminates," *International Journal of Machine Tools & Manufacture*, pp. 639–650, 1998.

[46] Josef Mayr , Jerzy Jedrzejewski , Eckart Uhlmann , M. Alkan Donmez ,

Wolfgang Knapp , Frank Hartig , Klaus Wendt , Toshimichi Moriwaki , Paul Shore ,Robert Schmitt , Christian Brecher , Timo Wurz , Konrad Wegener, "Thermal issues in machine tools," *CIRP Annals - Manufacturing Technology*, pp. 771–791, 2012.

[47] C. Emmelmann A. Goeke, "Influence of Laser Cutting Parameters on CFRP Part Quality," *Physics Procedia*, pp. 253–258, 2010.

[48] John C. Ion, *Laser Processing of Engineering Materials: Principles, Procedure and Industrial Application*.: Butterworth-Heinemann, March 2005.